Extracellular point mutations in FGFR2 elicit unexpected changes in intracellular signalling.

Zamal Ahmed[1], Annika C. Schuller[1], Klaus Suhling[2], Carolyn Tregidgo [2], & John E. Ladbury[1*]

[1]Department of Biochemistry and Molecular Biology, University College London, Gower Street, London WC1E 6BT, UK.

[2] Department of Physics, Kings College London, The Strand, London, WC2R 2LS, UK.

Running Title – Extracellular mutations affect FGFR2 intracellular signalling

Corresponding Author – John E. Ladbury, Department of Biochemistry and Molecular Biology, University College London, Gower Street, London WC1E 6BT, UK. Tel 020 7679 7012; Fax. 020 7679 7193; email j.ladbury@biochem.ucl.ac.uk.

Key Words – Aperts syndrome, signal transduction, FRS2, tyrosine kinase, FGFR2, FLIM, MAP kinase, lysosome, endocytosis, S252W and P253R point mutations, systems biology

Abstract

An understanding of cellular signalling from a systems-based approach has to be robust to the effects of point mutations in component proteins. Outcomes of these perturbations should be predictable in terms of downstream response otherwise a holistic interpretation of biological process or disease states cannot be obtained. Two single, proximal point mutations (S252W and P253R) in the extracellular region of FGFR2 prolong growth factor engagement resulting in dramatically different intracellular phenotypes. Following ligand stimulation the wild type receptor undergoes rapid endocytosis into lysosomes, whereas ^{SW}FGFR2 and ^{PR}FGFR2 remain on the cell membrane for extended period of time, modifying protein recruitment and elevating downstream ERK phosphorylation. FLIM reveals that direct interaction of FRS2 with wild type receptor occurs primarily at the vesicular membrane while the interaction with the P253R receptor occurs exclusively at the plasma membrane. These observations suggest that the altered FRS2 recruitment by the mutant receptors results in an abnormal cellular signalling mechanism. In this study these profound intracellular phenotypes resulting from extracellular modification reveal a new level of complexity which will challenge a systems biology interpretation.

Introduction

Fibroblast growth factor (FGF) receptors (FGFRs) are receptor tyrosine kinases involved in proliferation, growth inhibition and differentiation in different cell types [1]. All members of the FGFR family have an extracellular ligand-binding region, a transmembrane domain and an intracellular tyrosine kinase (TK) domain. The extracellular portion of the FGFRs (which comprises three immunoglobulin-like domains) interacts with the FGF ligands. So far 23 distinct FGFs have been identified in a variety of organisms [2,3]. Each FGFR isoform has restricted tissue-specific expression and ligand binding properties [1]. The growth factors alone are poor ligands for FGFRs without the cell surface accessory molecules heparan sulfate proteoglycans (HSPGs) [1,4,5]. The crystal structures of receptors bound to growth factors suggest that HSPGs form part of a ternary complex performing a dual function as both an augmenter of the FGF-FGFR interaction and a promoter of FGF-FGFR dimerization [6,7]. Receptor dimerization leads to autophosphorylation of seven conserved intracellular tyrosine residues [8] which serve as recruitment sites for SH2 domain-containing proteins to initiate downstream signalling [9]. The fibroblast growth factor receptor substrate 2 (FRS2) has been shown to be constitutively bound to FGFR1 [10]. On phosphorylation FRS2 serves as docking site for a number of intracellular proteins including Grb2 [11], SHP2 [12,13] and c-Cbl [14]. The recruitment of the Ras activator SOS through a Grb2/FRS2 complex is thought to be the primary route for activation of the MAP kinase pathway.

This work examines the effects of perturbing the growth factor binding, particularly with respect to the longevity of interaction. To assess how changing the temporal parameters of receptor signalling affects downstream, intracellular response we made two point mutations (S252W and P253R) in the linker region between the second and third immunoglobulin (Ig)-like domains of the extracellular portion of FGFR2. These mutations had previously been shown the give rise to higher affinity binding derived primarily from extended off rates for some FGF ligands, resulting in prolonged receptor engagement [15-17] and result in the phenotypically well characterised Apert syndrome [1,18-21]. X-ray crystallographic detail on the complexes of wild type and mutants of FGFR2 with FGF reveal that there are no gross conformational changes of the interacting proteins on complex formation, and the mutations impose limited changes to the receptor-growth factor interface [15-17]. Thus this receptor system provides an ideal model to probe the question of how a single point mutation which alters the temporal engagement of the growth factor affects protein interactions in intracellular signaling [22].

Using stable HEK293T cells transfected with wild type, S252W or P253R FGFR2 as our model we investigated differences in intracellular response to FGF binding. Comparison of the WT and mutant receptors reveal strikingly distinct temporal and spatial distribution of the ligand-activated receptor and the receptor-associated tyrosine phosphorylated proteins. Perhaps more surprising is the observation of idiosyncratic behaviour resulting from the individual mutants. The two mutant receptors appear to show altered glycosylation patterns and ligand-stimulated phosphorylation, as well as markedly up-regulated downstream signalling compared to the wild type FGFR2. In addition, FRS2

shows clear differences in localisation patterns and mode of interaction with the three receptors. This work emphasises the complex intracellular outcome resulting from limited modification to the extracellular domain and alteration of the time of engagement of the growth factor. This example suggests that since a dramatic perturbation of the intracellular signal transduction can arise from such a modest change to the receptor, the ultimate description of signalling from a systems biology perspective will be extremely challenging.

Experimental Procedures

Materials

Mouse monoclonal antibody directed against phosphorylated ERK and rabbit polyclonal antibody against total ERK were purchased from Cell Signaling Technology. A goat polyclonal antibody to GFP was purchased from Rockland Immunochemicals Inc. Anti-phosphotyrosine antibody (pY99), anti FGFR2 (Bek), anti-Grb2 (rabbit polyclonal), anti-FRS2 (rabbit polyclonal) and anti-tubulin were purchased from Santa Cruz Biotechnology. A mouse monoclonal anti-FRS2 was also purchased from R&D Systems. The pY99 anti-phosphotyrosine antibody was labelled with the sulphonamide dye Cy3 (Amersham Pharmacia) as described previously [23]. For the labelling of specific molecules a Cy3 antibody was used (molar ratio of 20:1). Tunicamycin was purchased from Calbiochem. LysoTracker Red DND99 was purchased from Invitrogen. GST-p13^{suc1} was purchased from Upstate.

Cloning

The full length FGFR2 (IIIc) and S252W cDNA were a gift from John Heath (University of Birmingham, UK) and was PCR amplified using flanking primers with BamHI and HindIII restriction sites. The amplified DNA was inserted in frame into the BamHI/HindIII site of the pEGFP-N2 vector (Clontech). The P253R mutations was created using a site directed mutagenesis kit (Stratagene) and confirmed by DNA sequencing. The WTΔE (similar to the K-*sam*-IIC3) was generated using an internal restriction site within the FGFR2 cDNA. The wild type FGFR2 in pEGFP was digested

with EcoRI/BamHI to remove 180 base pair DNA fragment from the C-terminus of the receptor. The monomeric red fluorescent protein (mRFP-C) in pcDNA3.1(+) was provided by Tony Ng (King's College London, UK) [24]. The full length human FRS2 cDNA (accession number: BC021562 (IMAGE: 4556225)) was obtained from HGMP, PCR amplified using flanking primers and subcloned in-frame into the mRFP-C vector.

Cell Culture

HEK293T, Hela and 3T3-L1 fibroblast cells were maintained in DMEM supplemented with 10% FBCS in a humidified incubator with 5% CO_2. ROS17/2.8 osteosarcoma cells were grown in phenol red free DMEM supplemented with 10% FBS and antibiotic. HEK293T Cells were transfected with DNA containing the ^{WT}FGFR2-GFP, ^{S252W}FGFR2-GFP or ^{P253R}FGFR2-GFP using Lipofectamine 2000 (Invitrogen) according to the manufacturer's instructions. Stable cells were generated by G418 selection (800µg/ml) for two weeks with a change of media every four days. The resulting antibiotic-resistant cells were plated in 96 well plates in limiting dilution. Individual wells with varying degrees of fluorescence were selected and expanded. Cells with equivalent levels of receptor were selected for comparison experiments. FRS2-RFP was transiently transfected into 293T cells over-expressing ^{WT}FGFR2-GFP, ^{S252W}FGFR2-GFP or ^{P253R}FGFR2-GFP respectively using Lipofectamine 2000 as before. 24 hours post-transfection cells were detached and seeded onto glass cover slips and allowed to grow for a further 48 hours before serum starvation and stimulation.

Cell Lysis, Immunoblotting and Pulldowns

Cells were grown in 10 cm dishes, serum starved overnight and then stimulated by addition of 10 ng/ml FGF2 or FGF9 (Peprotech or R & D Systems) and were incubated at 37 °C for the indicated time period. For tunicamycin treatment, cells were seeded and allowed to attach overnight, incubated with 3 or 10µg/ml tunicamycin for 18 hours and then lysed. Cells were lysed in lysis buffer containing 50 mM Hepes, pH 7.5, 1% (v/v) IGEPAL-C630, 1 mg/ml bacitracin, 1 mM EDTA, 10 mM NaF, 1 mM sodiumorthovanadate, 10% (v/v) glycerol, 50 mM NaCl, 1 mM PMSF and Protease Inhibitor Cocktail Set III (Calbiochem). The detergent-insoluble materials were sedimented by centrifugation at 13000 rpm for 15 min at 4 °C. 500 µg of cell lysate were used to precipitate FRS2 using anti-FRS2 antibody. Immunoblots were visualized with enhanced chemiluminescence (ECL). Images were analyzed with Fuji LAS-1000 Luminescent Image Analyser and quantitated with Fuji Image Gauge software.

Cell Imaging

Cells were seeded on glass coverslips 24 to 48 hours prior to stimulation. Serum starved cells were stimulated with 10 ng/ml FGF9 for the indicated time periods. Stimulation was stopped by transfer of the coverslip to 4% paraformaldehyde (pH 8.0). The pH in all subsequent steps was kept above 8.0. For antibody labelling cells were permeabilised with 1% saponin in PBS for 5 minutes at 4°C, washed with PBS and incubated with blocking solution (3% BSA/1% saponin/5% FCS in TBS) for 30 minutes at room temperature. The Cy3 labelled antibody was diluted in incubation buffer (3% BSA/1% saponin in TBS) and incubated overnight at 4°C. After washing in TBS for 4-5 times, the

coverslip was mounted on a slide with mounting media (0.1% p-phenylenediamine/50% glycerol in PBS at pH 7.5-8.0).

Microscopy

Confocal laser microscopy was performed with a Leica TCS SP system with a 63x oil immersion objective. GFP was excited with an argon visible light laser tuned to 488 nm, RFP and Cy3 with a krypton laser tuned to 568 nm. GFP and Cy3 or RFP were detected via 514/10 nm and 595/10 nm band selection respectively. Fluorescence images were collected using a photomultiplier tube interfaced to an Intel Pentium II system running Leica TCS NT control software. Co-localisation graphs were generated using the quantification function of the Leica NT software.

Fluorescence Lifetime Imaging Microscopy (FLIM)

Experiments were performed using an inverted confocal microscope (Leica TCS SP2) which was adapted for Time-Correlated Single-Photon Counting (TCSPC) FLIM with a Becker & Hickl SPC 830 card using 64 or 256 time channels in a 3 GHz, Pentium IV, 1GB RAM computer running Windows XP. The samples were excited with a femtosecond Titanium Sapphire laser (Coherent Mira, repetition rate 76 MHz.), pumped by a 6.5 W solid state laser (Coherent Verdi V6). Images were obtained with a line scan speed of 200 Hz, with an image size of 512 × 512 pixels. We used a 63× water immersion objective (numerical aperture NA=1.2) On the FLIM system the pixels were reduced to 256 × 256. The wavelength used for 2-photon excitation was 900 nm, and the fluorescence was detected through a 525+/-25nm interference filter using a cooled PMC100-01 detector (Becker & Hickl, based on a Hamamatsu H5772P-01

photomultiplier). The fluorescence decays were fitted with a single exponential decay model using Becker & Hickl's SPCImage software v2.8.3, and the GFP fluorescence lifetimes displayed in a false colour map.

Results

The expression and characterization of functional GFP tagged FGFR2 receptors

To identify a suitable model system a number of cell-lines, including some osteoblastic and fibroblastic cells, were screened. Two criteria were stipulated for the cell line; 1) there should be no endogenous FGFR2 expression, and 2) it must be able to express a sufficient quantity of transfected protein for high-quality microscopic imaging. Although a number of cell-lines met the first criteria they failed to stably express sufficient levels of exogenously introduced FGFR2. HEK293T cells proved to be an ideal model cell line since they lack endogenous FGFR2 and they express a sufficient quantity of tagged-FGFR2 allowing cellular imaging data to be obtained with clarity. Stable cell lines over-expressing wild type, S252W or P253R FGFR2 fused to GFP (hereafter referred to as ^{WT}FGFR2, ^{SW}FGFR2 and ^{PR}FGFR2 respectively) were established. Fluorescence images of cells show that all three fusion proteins were found predominantly in the plasma membrane, confirming that the GFP fusion did not interfere with receptor localization. There is a possibility that the GFP fusion construct and/or over-expression of the FGFR2 in the HEK293T cells induces dimerization of the receptor molecules and thereby constitutively activates the receptor. However, since we are comparing the differences in signalling between the wild type and the two mutants we expect any dimerization or constitutive activation effect would apply equally to all three receptors. To ensure that any observed differences in intracellular signalling were due to the receptor mutation, cell

lines with equivalent levels of receptor expression were obtained. A number of individual cell clones from each receptor cell-pool were obtained by limiting dilution and analysed by immunoblotting. Three individual cell lines expressing the WT and the two mutant receptors were probed with an antibody against GFP and showed an equivalent level of receptor expression on SDS-PAGE gels (Figure 1A upper panel). Furthermore multiple clones of each receptor were analysed for the downstream MAP kinase response to rule out any clonal genotypic variation between the individual cell-clones (data not shown). The receptors with extracellular point mutations show similar migration patterns to that of the wild type except that the major bands are gel shifted to a slightly higher molecular weight. Treatment of the cells with SU5402 (a specific inhibitor of FGFR kinase [25] inhibited the FGFR2 function but had negligible effect on the receptor mobility on SDS gel suggesting that the observed gel-shift with the mutant receptors is not due to increased phosphorylation (data not shown). The apparent increase in molecular weight of the bands for the ^{SW}FGFR2 and ^{PR}FGFR2 compared to wild type may report on additional receptor glycosylation. Inhibition of glycosylation using tunicamycin renders all three receptors to adopt a single identical molecular weight band on SDS gel (Figure 1B). We evaluated and quantified the extent of over-expression of these receptors in 293T cells in comparison to the endogenous level of the FGFR2 expression in a rat osteosarcoma cell line ROS17/2.8 (Figure 1C). Serially diluted total lysates of 293T cells over-expressing ^{WT}FGFR2 were loaded with the ROS17/2.8 cell lysate and immunoblotted using anti-FGFR2 antibody. The band intensities were quantified using densitometry and suggest that there is an approximate fourfold increase in the level expression in the transfected cells compared to the ROS17/2.8 cells.

To establish that the expressed receptors were functional as tyrosine kinases, the wild type and the mutant receptors were immunoprecipitated from FGF9-stimulated cells using an anti-GFP antibody, immunoblotted with an anti-phosphotyrosine antibody and quantified by densitometry (Figure 1D). Although all three cell-lines were serum starved under the same conditions and appear to express similar levels of receptors, cells expressing the ^{WT}FGFR2 and ^{PR}FGFR2 exhibit a higher level of basal receptor tyrosine phosphorylation than those with ^{SW}FGFR2. This suggests that the S252W point mutation somehow impedes background phosphorylation. The observed high level of basal receptor phosphorylation in ^{WT}FGFR2 and ^{PR}FGFR2 is not due to the GFP-fusion since transiently expressed non-tagged receptors portrayed a similar basal phosphorylation pattern (data not shown).

We next compared the effects of the expression of wild type and the two mutant receptors on cellular tyrosyl phosphoproteins. Immunoblotting with anti-phosphotyrosine antibody reveals that in cells expressing the S252W and the P253R receptors FRS2 undergoes robust tyrosine phosphorylation (Figure 1E top panel). The phosphorylation of FRS2 is minimal in cells expressing the wild type FGFR2. In the S252W cells FRS2 phosphorylation is apparent at 30 minutes post-stimulation while in the P253R cells the phosphorylation can be seen within 15 minutes of stimulation. Re-probing of the blot with anti-FRS antibody shows that although no tyrosine phosphorylation was observed in the cell expressing ^{WT}FGFR2, there is a stimulation dependent gel-shift of FRS2.

The ligand-dependent increase in protein phosphorylation is indicative of receptor kinase activity. Thus due to higher affinity/prolonged binding of the FGF-ligand, it might be expected that more mutant receptor molecules at the cell surface were engaged and activated by the ligand, thereby causing an overall increase in observed receptor phosphorylation. This is indeed true for the ^{SW}FGFR2 (Figure 1D), However both the wild type and the P253R receptors show similar levels of ligand-stimulated receptor phosphorylation and hence kinase activity (Figure 1D). So despite also having an increased affinity for FGF-ligand, the P253R mutant does not portray the same ligand-stimulated increase in receptor phosphorylation as the S252W receptor. This might be explained by the observation that the P253R mutant shows high levels of basal phosphorylation which could counteract the effect of increased affinity. The mutations therefore appear to have an effect on both basal and ligand-stimulated receptor phosphorylation in these cells. We currently hypothesise that this may result from effects on the C-terminus of the wild type receptor, since a deletion of the wild type receptor (similar to the K-sam-IIC3 deleted receptor [26]) resulted in a drastic reduction of the basal receptor phosphorylation (Figure 1F). The C-terminus of the FGFR2 contains several non-conserved tyrosine residues that may act as auto-substrate. Interestingly, the C-terminal deletion resulted in a lower level of tyrosine phosphorylation in the middle receptor band which accounts for most of tyrosine phosphorylation in absence of ligand in the wild type receptors (Figure 1F – exposure 2). This lack of the intermediatory receptor band phosphorylation is very similar to what is seen for the S252W receptor.

Spatial/temporal distribution of the tyrosine phosphorylated receptor and cellular phosphoprotein.

To assess the effect on receptor kinase activity of the extended engagement of FGFR2 by FGF we investigated differences in spatial and temporal distribution of tyrosine phosphorylated protein. Serum starved cells were stimulated over increasing periods of time with FGF9, fixed, permeabilised, stained with an anti-pY antibody coupled to Cy3, and observed by confocal microscopy. FGF9 was used in these experiments (as opposed to FGF2) because this ligand reported to be more specific for FGFR2 (IIIc) [15,27,28]. The specific nature of FGF9 for FGFR2 can also be exemplified in PC12 cells. These endogenously express FGFR1 and can be differentiated to form neurite extensions by FGF1 or FGF2 stimulation but not with FGF9. Exogenous expression of the FGFR2 in these cells and the subsequent FGF9-stimulation results in neuronal differentiation. This suggests that this growth factor can be used as a specific ligand for FGFR2 activation [29]. Cellular images of the wild type and mutant receptors, and total tyrosine-phosphorylated protein pre- and post-FGF9 stimulation are shown in Figure 2. Prior to stimulation ^{WT}FGFR2 resided predominantly in the plasma membrane and limited amounts of tyrosine phosphorylated proteins co-localised with the receptor (Figure 2A ^{WT}FGFR2 basal image and graph). Although this level of basal receptor phosphorylation appears to be contradictory to the observation in Figure 1C, closer inspection of all the sections of the cell image revealed large amount of receptor co-localized with tyrosine phosphorylated protein in sections closest to the glass slide. Five minutes after the addition of FGF9 some intermittent intracellular vesicular clusters containing receptors that are tyrosine phosphorylated, or localised with phosphorylated protein were observed

(data not shown). This population increased at 15 minutes (Figure 2A ^{WT}FGFR2 15 min image). A graphical representation of the fluorescent intensity through a cross-section of the cell confirms that the receptor on the plasma membrane at 15 minutes post-stimulation was minimally tyrosine phosphorylated and/or did not co-localise with cellular tyrosine phosphorylated proteins. The presence of unphosphorylated receptor can be seen as single green peak (i.e. without the equivalent red peak corresponding to the phosphorylated protein) at the point where the line drawn in the overlaid image crosses the membrane (Figure 2A. and 15 min. graphs). This demonstrates that phosphorylated receptor appears to be rapidly internalised post-stimulation. At 60 minutes the receptors that were found at the cell membrane appeared to be either tyrosine phosphorylated or co-localized with tyrosine phosphoproteins (Figure 2A ^{WT}FGFR2 60 min image). As a control experiment cells were stimulated with 100ng/ml insulin. This shows little effect on the FGFR2 receptor localization but widespread phosphoprotein-containing vesicles were observed (Figure 2B).

In cells expressing ^{SW}FGFR2 the receptor resides predominantly at the cell membrane with a low level of phosphorylation or co-localization with tyrosine phosphorylated proteins before stimulation (Figure 2A. basal image and graph). Following FGF9 stimulation an increase in the phosphorylation of the receptor, or concentration of proximal tyrosine phosphorylated proteins on the membrane was observed with time. At 15 minutes post-stimulation it is apparent that the ^{SW}FGFR2 do not undergo the same degree of endocytosis as seen with the wild type receptors (seen in approximately 90% of cells (Figure 2A ^{SW}FGFR2 15min). However, some punctate clusters do appear at 60

minutes but far less than that seen with the wild type receptor (Figure 2A ^{SW}FGFR2 60min). Thus the S252W mutation seems to restrict and/or delay the normal endocytic process and thereby also interfere with endocytosis of phosphorylated protein. The fact that vast majority of the receptor and tyrosine phosphorylated protein localise to the plasma membrane as opposed to the intracellular vesicles seen with the wild type receptor suggest a serious alteration of spatial, and to some extent temporal signalling by the S252W mutant receptor.

Cells expressing ^{PR}FGFR2 showed some clustering of phosphorylated receptors or tyrosine phosphorylated proteins at the cell-membrane in the basal state (Figure 2A ^{PR}FGFR2 basal graph). After FGF9 stimulation receptors on the plasma membrane were tyrosine phosphorylated or associated with phosphoprotein (Figure 2A ^{PR}FGFR2 15min). Although there was a progressive time-dependent increase of receptor phosphorylation on the cell membrane, a number of intracellular vesicles with receptors were also seen at 60 minutes (Figure 2A ^{PR}FGFR2 60min). This is similar to the S252W mutant where a delayed and limited number of receptor and phosphoprotein-containing vesicles was observed. This suggests both mutants share a similar internalisation pattern and therefore would generate similar signalling complexes primarily on the cell membrane that could give rise to an altered mechanism of signalling.

MAP kinase activation

Having observed the altered spatio-temporal patterns of receptor and cellular phosphoprotein localization between the mutants and the wild type receptors we chose to investigate the effect of these two mutations on downstream cellular response. One of the

downstream effectors of FGF receptors is the MAP kinase, ERK which plays an essential role in mitogenesis [1,30]. Thus differences in the level of ERK phosphorylation would provide an insight into how the altered spatial-temporal receptor distributions of S252W and P253R mutations affect the downstream signalling events. Cells were serum starved overnight and stimulated with 10ng/ml FGF2 or FGF9. Cell lysates were immunoblotted against phosphorylated ERK (Figure 3A upper panel), stripped and re-probed against total ERK (Figure 3A. lower panel). Phospho-ERK immunoblots from three independent experiments were quantified using densitometry. FGF2 and FGF9 (Figure 3B. and C respectively) stimulation resulted in a time-dependent increase in the ERK activation in all three cell lines which was sustained over the 60 minute time course. Cells expressing the FGFR2 with the mutations displayed enhanced FGF2 and FGF9 stimulated ERK phosphorylation in comparison to the wild type. Similar ERK phosphorylation patterns were observed in FGF2 stimulated ROS17/2.8 cells and FGF9 stimulated PC12 cells over-expressing the wild type and mutant receptors (data not shown). This suggests that the observed altered receptor distribution in Figure 2 has a profound effect on the downstream receptor signalling as demonstrated by the enhanced MAP kinase response. This observation underscores the pivotal role of receptor downstream response which was demonstrated in a recent study with mouse model of Apert syndrome where inhibition of MAPK relieved craniosynostosis and premature fusion of coronal suture and restored normal body mass [31].

Cellular localization of FRS2

FRS2 has been shown to play a major role in the recruitment of the Grb2/SOS complex to the FGFR1 and in the subsequent downstream activation of the MAP kinase pathway

[11,32]. In order to understand the cellular signalling process, we investigated whether the differences in MAP kinase activation observed for FGFR2 and mutants thereof arose as a result of differential recruitment of FRS2. This was assessed by comparing the localization of C-terminally RFP-tagged FRS2 in cells expressing GFP-tagged WT or mutant receptors (Figure 4). Prior to FGF stimulation FRS2 shows perfect co-localization with the wild type receptor on the cell membrane (Figure 4A ^{WT}FGFR2 basal image and graph). This is in contrast to expression of RFP alone which shows diffused distribution throughout the cell (Figure 4B). At 15 minutes post-FGF9 stimulation intracellular vesicles containing both FGFR2 and FRS2 were observed (Figure 4A ^{WT}FGFR2). By 60 minutes in >90% of cells the majority of the vesicles had dissipated and both FGFR2 and FRS2 re-appear at the plasma membrane (Figure 4A ^{WT}FGFR2 60min image and graph). Therefore, the ^{WT}FGFR2 and FRS2 undergo transient ligand-dependent endocytosis. As expected in a control using insulin stimulation of these cells, little effect on the cellular localization of the FGFR2 and FRS2 was observed (Figure 4B).

In resting cells expressing the S252W mutant, both the receptor and FRS2 show membrane co-localization (Figure 4B ^{SW}FGFR2 basal image and graph). Unlike in the wild type cells however, most FRS2 and ^{SW}FGFR2 molecules continue to reside on the cell-membrane throughout the stimulation time period (Figure 4B 15 and 60 min.). This is consistent with the earlier observation of phosphorylated ^{SW}FGFR2 and/or other phosphorylated protein remaining on the membrane for an extend period of time (Figure 2A). Interestingly, FGF9 stimulation of ^{SW}FGFR2 induced the formation of intracellular vesicles containing only FRS2 this is in contrast to the wild type receptor suggesting

distinct modes of FRS2 processing (Figure 4B ^{SW}FGFR2 at 15 and 60 min graph, arrows showing intense FRS2-RFP peak only). The observed receptor independent FRS2 vesicles may be caused by the inability of the S252W receptor undergo prompt endocytosis.

The ^{PR}FGFR2 exhibits yet another apparent co-localization pattern with FRS2. Like the ^{WT}FGFR2 and ^{SW}FGFR2, at basal state, both the receptor and FRS2 co-localize at the plasma membrane (Figure 4C ^{PR}FGFR2 basal image and graph). However, unlike the other receptors, very few intracellular vesicles containing FRS2 and the receptor (as seen with ^{WT}FGFR2), or FRS2 alone (as seen with the ^{SW}FGFR2) were formed throughout the period of stimulation (Figure 4C). The majority of the receptors and FRS2 remained on the membrane throughout the time course. This is consistent with the prolonged appearance of phosphorylated receptor (or recruited phosphoprotein) at the membrane after stimulation (Figure 2C ^{PR}FGFR2). The changes that occur in the ligand-receptor interaction as a result of the mutations completely alter the cellular localisation of FRS2. Since FRS2 is the main FGFR docking protein responsible for MAPK activation, the changes in its cellular localisation may contribute to the observed enhanced MAPK response shown in Figure 3.

Protein precipitation with FRS2

As the wild type and mutants show distinct patterns of cellular localisation with FRS2 we next investigated whether this had an impact on the assembly of the signalling complexes generated. FRS2 was immunoprecipitated from cells expressing the wild type and the mutant FGFR2 using an anti-FRS2 antibody. The precipitants were subjected to

immunoblotting with an anti-phosphotyrosine antibody (Figure 5A upper panel), stripped and re-probed with an anti-FRS antibody (Figure 5A upper middle panel), anti-FGFR2 (Figure 5A lower middle panel) and IgG (Figure 5A bottom panel). The unstimulated cells expressing the wild type FGFR2 receptor show very low levels of FRS2 phosphorylation and co-precipitation of receptors. This suggests that although the proteins co-localise at the cell membrane (seen in the overlay of the cell images, Figure 4A), they may not be interacting or are in a complexed state. Following FGF-stimulation, there is an increase in the level of FRS2 phosphorylation and co-precipitation of receptors (Figure 5A lane 2). In addition a number of cellular tyrosine phosphorylated proteins are seen to be in complex with the receptor and FRS2, most notably a protein of apparent molecular weight of 60kDa. Thus, in cells expressing the wild type receptor it appears that the association of FRS2 and the FGFR2 predominantly occurs in a stimulation-dependent manner.

In unstimulated ^{SW}FGFR2-expressing cells FRS2 is in complex with a number of highly phosphorylated cellular proteins (Figure 5A upper panel lane 3). Following FGF9 stimulation however, the amounts of cellular phosphoproteins in complex with FRS2 and co-precipitation of the receptor shows a slight reduction (Figure 5A upper panel, lane 4). This is different to the observation with the wild type receptor, where ligand stimulation led to an increase in tyrosine phosphorylated protein recruited to the receptor-FRS2 complex. However, the phosphorylation of the apparent 60kDa protein increases with FGF stimulation. In cells expressing the P253R mutant receptors phosphorylation of FRS2 remains virtually unchanged between unstimulated cells and FGF-stimulated cells.

Although a slight reduction in FGF stimulated complex formation by cellular phosphoproteins is seen, an almost equal level of receptors were co-precipitated from both unstimulated and FGF9-stimulated cells (Figure 5A, upper panel, lanes 5 and 6). Therefore, the P253R receptors appear to be constitutively associated or in a multi-protein complex with FRS2. The stimulation-dependent FRS2 tyrosine phosphorylation appears to be more robust in the mutants (Figure 5A upper panel and Figure 1E).

To confirm the observation of a lack of constitutive association of FGFR2 and FRS2 we also tested the stimulation-dependent association of FGFR2 with FRS2 in ROS17/2.8 cells. These cells express endogenous FGFR2. Serum starved cells were stimulated with FGF2 and FGF9 and cell lysates were prepared and pulled down with GST-p13^{suc1}. The pulldown experiment was performed because the FRS2 antibody preformed poorly in ROS cells. The precipitants were subjected to immunoblotting with an anti-phosphotyrosine antibody (Figure 5B upper panel), stripped and re-probed with an anti-FGFR2 (Figure 5B upper middle panel), anti-FRS2 (Figure 5B lower middle panel) and anti-GST antibodies (Figure 5B bottom panel). There was an apparent stimulation-dependent receptor co-precipitation with FRS2 similar to the observation in FGFR2 transfected 293T cells.

Direct interaction of FRS2 with the wild type and mutant receptors.

Although immunoprecipitation can be an indication of direct interaction, co-precipitation can also occur due to the formation of ternary complexes with other cellular proteins. Since the FRS2 pulldown and the co-localisation studies suggested differences in FRS2 recruitment to the receptor, FLIM (fluorescence lifetime imaging microscopy) was

chosen to unambiguously investigate whether these differences were the result of altered direct interaction [24,33,34]. FLIM has successfully been used to show direct interactions of proteins in cells [24]. Upon excitation, if the donor GFP (which is fused to FGFR2) is within the critical distance of 10 nm of an acceptor RFP (which is tagged to a target protein, i.e. FRS2) Förster resonance energy transfer (FRET) occurs from the donor to the acceptor. This results in a reduction of the emission lifetime of the donor molecule (GFP) which is measurable and indicates a direct interaction between the two molecules. The use of FLIM to detect FRET can be very accurate and has the advantage that only the GFP donor fluorescence needs to be measured.

At basal state there are a few isolated clusters in which interaction between the ^{WT}FGFR2 and FRS2 can be observed (Figure 6A, basal lifetime image). This low level of FRS2-FGFR2 interaction seems to have little effect on the average lifetime graph where the peak is centred on approximately 2.0 ns (similar to that for isolated GFP; Figure 6A basal and 6D) and cells expressing only the GFP-tagged wild type receptor (data not shown). On FGF9 stimulation a large population of punctate intracellular vesicle clusters show very short lifetimes, indicative of a direct interaction (Figure 6A, 15 minute lifetime graph: peak shifts to left). This corroborates previously described evidence for rapid dissipation of receptor and FRS2 from the membrane on stimulation (Figure 2A and 4A respectively). FRS2 and FGFR2 appear to be no longer engaged in direct interaction at 60 minutes (Figure 6A). Therefore, from these data we can conclude that the wild type receptor interacts with FRS2 transiently in vesicles in a receptor activation-dependent manner and the interaction eventually dissociates with sustained ligand activation.

A high level of basal interaction was observed between ^{SW}FGFR2 and FRS2 (blue coloration in the lifetime image and the shorter average lifetime of the population at 1.7ns (Figure 6B). This level of association appears to be partly lost on FGF9 stimulation (average lifetime closer to 2.0 ns i.e. graph shifts to the right; Figure 6B, 15 and 60 min.). This observation correlates with the anti-FRS2 immunoprecipitation experiment (Figure 5A) where ligand stimulation showed a decrease in the ^{SW}FGFR2 and cellular phosphoprotein co-precipitation with FRS2. The loss of direct FRS2 association with the S252W receptor upon FGF9 stimulation further correlates with the previously observed stimulation-dependent sequestering of FRS2 into independent vesicles (Figure 4B). Therefore, like the FGFR1, FRS2 is constitutively associated with ^{SW}FGFR2 however, ligand stimulation of the mutant receptor leads to the dissociation of this interaction. This is the opposite of the observation in cells expressing the wild type receptors where ligand stimulation leads to the formation of FRS2-receptor interactions.

The P253R mutant, like the S252W receptor, showed direct interactions between the receptor and FRS2 at basal level. However, unlike the S252W receptor but similar to the wild type receptor, FGF9 stimulation results in an increase in P253R-FRS2 interaction (graph peak shifts to the left Figure 6C). However at 15 minutes all interactions between the P253R receptor and FRS2 occur exclusively at the plasma membrane (Figure 6C, 15 minutes lifetime image and graph). This is again consistent with the previously observed co-localisation of ^{PR}FGFR2 with FRS2 (Figure 4C). The combined FLIM data suggest that all three receptors are involved in profoundly different interactions with FRS2. The

^{WT}FGFR2 and ^{PR}FGFR2 display stimulation-dependent interaction with FRS2 in the plasma and vesicular membranes respectively. The ^{SW}FGFR2, on the other hand, shows direct constitutive interaction with FRS2 on the plasma membrane.

Wild type FGFR2 localizes to lysosome.

Throughout the course of this investigation it was apparent that the wild type FGFR2 undergoes ligand-stimulated receptor endocytosis into intracellular vesicles while the mutant receptors are resistant to this process. This suggests endocytosis into intracellular vesicles is a fundamental signalling difference between the wild type and the two mutant receptors. Endocytosis plays pivotal role in activation or down-regulation of many receptor tyrosine kinases. In an effort to identify the intracellular vesicle to which FGFR2 is processed we probed cells with various vesicle markers including those for endosomes, caveolae and lysosomes. The vast majority of the ligand-stimulated endocytosed receptors co-localize with lysosomal marker (Figure 7) (it should be noted that the lysosomal marker used in this study is dye that detects low pH level and therefore could also detect late endosomes). In unstimulated cells the FGFR2 do not co-localize with the marker (Figure 7 a, d and g), however on FGF9 stimulation a number of vesicles containing the receptor were co-stained (Figure 7 b, e and h). Further ligand stimulation resulted in virtually all of the receptors being identified as being localised with the lysosomal marker (Figure 7 e, f and i). Lysosomes are specialised organelles containing degradative enzymes with an internal pH of 4.8. Therefore localization of the receptor to the lysosome would have one the two possible outcomes; degradation of the receptors by the residence proteases and/or dissociation of the ligand from the receptor due to the low

pH environment. Nevertheless either process would result in receptor down-regulation. In contrast to the ^{WT}FGFR2, the two mutant receptors show drastic reduction in their ability to endocytose to lysosomes thus we would expect the observed relative enhanced MAP kinase response (Figure 3).

Discussion

Previous studies have suggested that prolonged receptor engagement and altered specificity for growth factors are the only outwardly discernable consequence of the S252W and P253R point mutations [15,16,35,36]. It is thus remarkable to observe such dramatic changes in the properties of the receptor molecules defined by clear differences in glycosylation, phosphorylation, direct interaction with FRS2, and downstream MAP kinase activity. In addition, bearing in mind the proximity of the point mutations and the structurally subtle nature of the changes which these produce in growth factor recognition, it is also intriguing to observe the profound changes in functional properties between ^{SW}FGFR2 and ^{PR}FGFR2 themselves.

The receptors appear as more than one band on an immunoblot, which most likely reflects differences in glycosylation. It is not clear mechanistically how this altered glycosylation might impinge on intracellular signalling, and there is no structural basis for glycosylation affecting the interface between FGF and FGFR2. Total ablation of glycosylation can result in a decrease in ligand-independent dimerisation and phosphorylation [37]. However, the wealth of data on the direct interaction between FGF and the extracellular domain of FGFR2 infer that the effect of N-glycosylation can largely be ignored [16].

One key feature of the point mutations in the receptors which is independent of the time of growth factor engagement is the observed difference in levels of basal phosphorylation. Whilst wild type and ^{PR}FGFR2 are highly phosphorylated, ^{SW}FGFR2 is significantly less so (Figure 1E). As a result the effect of stimulation appears as a dramatic increase in phosphorylation of ^{SW}FGFR2; this is less profound on the other two receptors (Figure 1D). This demonstrates a clear phenotypic alteration between the mutant receptors themselves. A striking difference between the S252W and the P253R is that the S252W has an apparent higher molecular weight which could be viewed as a more 'matured' form and correlates with reduced basal phosphorylation. The wild type and the P253R contain more of the intermediate form of the receptors which shows higher level of basal phosphorylation. The C-terminus of the receptor appears to play a vital part in the 'maturity' of receptors. The C-terminal truncated receptor shows less basal receptor phosphorylation compared to the wild type suggesting that it might play a part in receptor processing (Figure 1F).

On stimulation a further clear phenotypic difference between the cells expressing the different receptors was apparent. The absence of phosphorylated ^{WT}FGFR2 on the cell membrane (Figure 2) and its appearance in vesicles suggests that normal FGFR2 signalling involves endocytosis of the receptor once ligand is bound. In contrast, the phosphorylated mutant receptors and/or subsidiary phosphoproteins seem to remain at the membrane throughout the 60 minute time course (Figure 2A). Thus the prolonged engagement of the receptors expressing the extracellular mutations confers some

inhibitory effect on the endocytic process. Since ligand-stimulated internalisation has been reported as playing a pivotal role in signal down-regulation for a number of other tyrosine kinase receptors, it is likely that the inability of the mutant receptors to undergo endocytosis may result in the apparent elevated levels of MAP kinase activity [4,38-42].

The prolonged receptor engagement by ligand results in a dramatic change in complex formation between FRS2 and the receptor. In unstimulated cells, all three receptors appear to co-localise with FRS2 (Figure 4). However, immunoprecipitation assays and FLIM (Figures 5A and 6A respectively) reveal that direct interaction with ^{WT}FGFR2 occurs only in isolated clusters, suggesting that although they all have the same spatial distribution, majority of the FRS2 is not interacting directly with the wild type receptor. This is intriguing in the light of the observation of a basal constitutive complex between FRS2 and FGFR1 [10] and suggests significant differences in early signalling complex protein recruitment between these receptors. Interestingly, very clear differences in direct interaction between the unstimulated mutant receptors and FRS2 were demonstrated by the lifetimes observed in the FLIM data, with ^{SW}FGFR2 being the most pronounced.

In cells expressing ^{WT}FGFR2 the phosphorylated FGFR2-FRS2 interaction occurs predominantly in the lysosome (Figures 6A and 7). The P253R mutant receptor complex prevails almost exclusively at the cell membrane (Figures 4 and 6). This is consistent with the observation of the distinct membrane localisation of phosphorylated ^{PR}FGFR2 receptor and/or phosphoprotein on stimulation (Figure 2 and Figure 5A). The level of direct interaction of ^{SW}FGFR with FRS2 declines following stimulation compared to the

other two receptors (Figure 6B) this is consistent with immunoprecipitation experiment where the S252W receptor and phosphoprotein precipitated by FRS2 shows a stimulation-dependent decrease (Figure 5A). Since each of the three receptors show different properties of spatial and temporal distribution with FRS2 it is likely that time of engagement and the ensuing localisation of the receptors dictates how signalling complexes are formed.

The Apert syndrome mutant receptors in the HEK293T cells provide a useful model system to show the dramatic effect of change in the temporal activity of signalling molecules. Indeed this work represents the first demonstration of the effects of modulating the time of receptor engagement through an identical ligand. The resulting changes observed with respect to receptor phosphorylation and localisation, protein recruitment, and downstream MAP kinase response strongly suggests that the time of receptor engagement is a fundamental determinant of specificity in intracellular signal transduction [22]. It is clear from this work that without invoking a time element to the definition of a signalling process, no real understanding of the ultimate outcome can be attained. Since the single point mutations result in dramatic change to the basic protein signalling mechanism in distinct ways, the chances of predicting these from a global knowledge and quantification of the process for the wild type are small. This argues that a holistic appreciation of tyrosine kinase-mediated signal transduction is likely to be a distant goal.

Acknowledgements

This work was funded by the Wellcome Trust. J.E.L is a Wellcome Trust Senior Research Fellow. A.C.S. is a Countess of Lisburne Scholar. We are indebted to J. Brockes and K. Bowers for their critical reading of the manuscript.

Abbreviations: FGFR, fibroblast growth factor receptor; FRS2, fibroblast growth factor receptor substrate 2; FLIM, fluorescent lifetime imagining microscopy; GFP, green fluorescent protein; RFP, red fluorescent protein.

References

1 Powers, C.J., McLeskey, S. W. and Wellstein, A. (2000) Fibroblast growth factors, their receptors and signaling. Endocr. Relat Cancer, **7,** 165-197.

2 ADHR Consortium. (2000) Autosomal dominant hypophosphataemic rickets is associated with mutations in FGF23. Nat. Genet., **26,** 345-348.

3 Ornitz, D. M. and Itoh, N. (2001) Fibroblast growth factors. Genome Biol., **2,** Reviews 3005.

4 Yayon, A., Klagsbrun, M., Esko, J. D., Leder, P. and Ornitz, D. M. (1991) Cell surface, heparin-like molecules are required for binding of basic fibroblast growth factor to its high affinity receptor. Cell, **64,** 841-848.

5 Spivak-Kroizman, T., Lemmon, M. A., Dikic, I., Ladbury, J. E., Pinchasi, D., Huang, J., Jaye, M., Crumley, G., Schlessinger, J. and Lax, I. (1994) Heparin-induced oligomerization of FGF molecules is responsible for FGF receptor dimerization, activation, and cell proliferation. Cell, **79,** 1015-1024.

6 Pellegrini, L., Burke, D. F., von Delft, F., Mulloy, B. and Blundell, T. L. (2000) Crystal structure of fibroblast growth factor receptor ectodomain bound to ligand and heparin. Nature, **407**, 1029-1034.

7 Schlessinger, J., Plotnikov, A. N., Ibrahimi, O. A., Eliseenkova, A. V., Yeh, B. K., Yayon, A., Linhardt, R. J. and Mohammadi, M. (2000) Crystal structure of a ternary FGF-FGFR-heparin complex reveals a dual role for heparin in FGFR binding and dimerization. Mol. Cell, **6,** 743-750.

8 Mohammadi, M., Dikic, I., Sorokin, A., Burgess, W. H., Jaye, M. and Schlessinger, J. (1996) Identification of six novel autophosphorylation sites on fibroblast growth factor receptor 1 and elucidation of their importance in receptor activation and signal transduction. Mol. Cell Biol., **16**, 977-989.

9 Schlessinger, J. (2000) Cell signaling by receptor tyrosine kinases. Cell, **103,** 211-225.

10 Ong, S. H., Guy, G. R., Hadari, Y. R., Laks, S., Gotoh, N., Schlessinger, J. and Lax, I. (2000) FRS2 proteins recruit intracellular signaling pathways by binding to diverse targets on fibroblast growth factor and nerve growth factor receptors. Mol. Cell Biol., **20,** 979-989.

11 Kouhara, H., Hadari, Y. R., Spivak-Kroizman, T., Schilling, J., Bar-Sagi, D., Lax, I. and Schlessinger, J. (1997) A lipid-anchored Grb2-binding protein that links FGF-receptor activation to the Ras/MAPK signaling pathway. Cell, **89,** 693-702.

12 Ong, S.H., Lim, Y. P., Low, B. C. and Guy, G. R. (1997) SHP2 associates directly with tyrosine phosphorylated p90 (SNT) protein in FGF-stimulated cells. Biochem. Biophys. Res. Commun., **238,** 261-266.

13 Hadari, Y. R., Kouhara, H., Lax, I. and Schlessinger, J. (1998) Binding of Shp2 tyrosine phosphatase to FRS2 is essential for fibroblast growth factor-induced PC12 cell differentiation. Mol. Cell Biol., **18,** 3966-3973.

14 Wong, A., Lamothe, B., Lee, A., Schlessinger, J. and Lax, I. (2002) FRS2 alpha attenuates FGF receptor signaling by Grb2-mediated recruitment of the ubiquitin ligase Cbl. Proc. Natl. Acad. Sci.U.S.A, **99,** 6684-6689.

15 Anderson, J., Burns, H. D., Enriquez-Harris, P., Wilkie, A. O. M. and Heath,J.K. (1998) Apert syndrome mutations in fibroblast growth factor receptor 2 exhibit increased affinity for FGF ligand. Hum.Mol.Genet., **7,** 1475-1483.

16 Ibrahimi, O. A., Eliseenkova, A. V., Plotnikov, A. N., Yu, K., Ornitz, D. M. and Mohammadi, M. (2001) Structural basis for fibroblast growth factor receptor 2 activation in Apert syndrome. Proc. Natl. Acad. Sci. U.S.A, **98,** 7182-7187.

17 Yu, K., Herr, A. B., Waksman, G. and Ornitz, D. M. (2000) Loss of fibroblast growth factor receptor 2 ligand-binding specificity in Apert syndrome. Proc. Natl. Acad. Sci. U.S.A, **97,** 14536-14541.

18 Cohen, M. M., Jr., Kreiborg, S., Lammer, E. J., Cordero, J. F., Mastroiacovo, P., Erickson, J. D., Roeper, P. and Martinez-Frias, M. L. (1992) Birth prevalence study of the Apert syndrome. Am. J. Med. Genet., 4**2,** 655-659.

19 Oldridge, M., Lunt, P.W., Zackai, E. H., Donald-McGinn, D. M., Muenke,M., Moloney, D. M., Twigg, S. R., Heath, J. K., Howard, T. D., Hoganson, G., Gagnon, D. M., Jabs, E. W. and Wilkie, A. O. M. (1997) Genotype-phenotype correlation for nucleotide substitutions in the IgII-IgIII linker of FGFR2. Hum. Mol. Genet., **6,** 137-143.

20 Oldridge, M., Zackai, E. H., Donald-McGinn, D. M., Iseki, S., Morriss-Kay, G. M., Twigg, S. R., Johnson, D., Wall, S. A., Jiang, W., Theda, C., Jabs, E. W. and Wilkie, A. O. M. (1999) De novo alu-element insertions in FGFR2 identify a distinct pathological basis for Apert syndrome. Am. J. Hum. Genet., **64,** 446-461.

21 Wilkie, A. O. M., Slaney, S. F., Oldridge, M., Poole, M. D., Ashworth, G. J., Hockley, A. D., Hayward, R. D., David, D. J., Pulleyn, L. J., Rutland, P. Malcolm, S., Winter, R. M., and Reardon, W. . (1995) Apert syndrome results from localized mutations of FGFR2 and is allelic with Crouzon syndrome. Nat. Genet., **9,** 165-172.

22 O'Rourke, L. and Ladbury, J. E. (2003) Specificity is complex and time consuming: mutual exclusivity in tyrosine kinase-mediated signaling. Acc. Chem. Res., **36,** 410-416.

23 Ahmed, Z., Beeton, C. A., Williams, M. A., Clements, D., Baldari, C. T. and Ladbury, J. E. (2005) Distinct spatial and temporal distribution of ZAP70 and Lck following stimulation of interferon and T-cell receptors. J. Mol. Biol., **353,** 1001-1010.

24 Peter, M., meer-Beg, S. M., Hughes, M. K., Keppler, M. D., Prag, S., Marsh, M., Vojnovic, B. and Ng, T. (2005) Multiphoton-FLIM quantification of the EGFP-mRFP1

FRET pair for localization of membrane receptor-kinase interactions. Biophys. J., **88**, 1224-1237.

25 Mohammadi, M., McMahon, G., Sun, L., Tang, C., Hirth, P., Yeh, B. K., Hubbard, S. R. and Schlessinger,J. (1997) Structures of the tyrosine kinase domain of fibroblast growth factor receptor in complex with inhibitors. Science, **276,** 955-960.

26 Itoh, H., Hattori, Y., Sakamoto, H., Ishii, H., Kishi, T., Sasaki, H., Yoshida, T., Koono, M., Sugimura, T. and Terada, M. (1994) Preferential alternative splicing in cancer generates a K-sam messenger RNA with higher transforming activity. Cancer Res., **54,** 3237-3241.

27 Eswarakumar, V. P., Lax, I. and Schlessinger, J. (2005) Cellular signaling by fibroblast growth factor receptors. Cytokine Growth Factor Rev., **16**, 139-149.

28 Ibrahimi, O. A., Zhang, F., Eliseenkova, A. V., Linhardt, R. J. and Mohammadi, M. (2004) Proline to arginine mutations in FGF receptors 1 and 3 result in Pfeiffer and Muenke craniosynostosis syndromes through enhancement of FGF binding affinity. Hum. Mol. Genet., **13,** 69-78.

29 Schuller, A. C., Ahmed, Z. and Ladbury, J. E. (2008) Extracellular point mutations in FGFR2 result in elevated ERK1/2 activation and perturbation of neuronal differentiation. Biochem. J., **410,** 205-211.

30 Dailey, L., Ambrosetti, D., Mansukhani, A. and Basilico, C. (2005) Mechanisms underlying differential responses to FGF signaling. Cytokine Growth Factor Rev., **16,** 233-247.

31 Shukla, V., Coumoul, X., Wang, R. H., Kim, H. S. and Deng, C. X. (2007) RNA interference and inhibition of MEK-ERK signaling prevent abnormal skeletal phenotypes in a mouse model of craniosynostosis. Nat.Genet., **39,** 1145-1150.

32 Wu, Y., Chen, Z. and Ullrich, A. (2003) EGFR and FGFR signaling through FRS2 is subject to negative feedback control by ERK1/2. Biol. Chem., **384,** 1215-1226.

33 Treanor, B., Lanigan, P.M., Suhling, K., Schreiber, T., Munro, I., Neil, M. A., Phillips, D., Davis, D. M. and French, P. M. (2005) Imaging fluorescence lifetime heterogeneity applied to GFP-tagged MHC protein at an immunological synapse. J. Microsc., **217**, 36-43.

34 Suhling, K., French, P. M. and Phillips, D. (2005) Time-resolved fluorescence microscopy. Photochem. Photobiol. Sci., **4,** 13-22.

35 Ibrahimi, O. A., Zhang, F., Eliseenkova, A. V., Itoh, N., Linhardt, R. J. and Mohammadi, M. (2004) Biochemical analysis of pathogenic ligand-dependent FGFR2 mutations suggests distinct pathophysiological mechanisms for craniofacial and limb abnormalities. Hum. Mol. Genet., **13,** 2313-2324.

36 Mohammadi, M., Olsen, S. K. and Ibrahimi, O. A. (2005) Structural basis for fibroblast growth factor receptor activation. Cytokine Growth Factor Rev., **16,** 107-137.

37 Hatch, N. E., Hudson, M., Seto, M. L., Cunningham, M. L. and Bothwell, M. (2006) Intracellular retention, degradation, and signaling of glycosylation-deficient FGFR2 and craniosynostosis syndrome-associated FGFR2C278F. J. Biol. Chem., **281,** 27292-27305.

38 Le, R. C. and Wrana, J. L. (2005) Clathrin- and non-clathrin-mediated endocytic regulation of cell signalling. Nat. Rev. Mol. Cell Biol., **6,** 112-126.

39 Haglund, K., Sigismund, S., Polo, S., Szymkiewicz, I., Di Fiore, P. P. and Dikic, I. (2003) Multiple monoubiquitination of RTKs is sufficient for their endocytosis and degradation. Nat. Cell Biol., **5,** 461-466.

40 Mosesson, Y., Shtiegman, K., Katz, M., Zwang, Y., Vereb, G., Szollosi, J. and Yarden, Y. (2003) Endocytosis of receptor tyrosine kinases is driven by monoubiquitylation, not polyubiquitylation. J. Biol. Chem., **278,** 21323-21326.

41 Peschard, P. and Park, M. (2003) Escape from Cbl-mediated downregulation: a recurrent theme for oncogenic deregulation of receptor tyrosine kinases. Cancer Cell, **3,** 519-523.

42 Waterman, H., Katz, M., Rubin, C., Shtiegman, K., Lavi, S., Elson, A., Jovin, T. and Yarden, Y. (2002) A mutant EGF-receptor defective in ubiquitylation and endocytosis unveils a role for Grb2 in negative signaling. EMBO J., **21,** 303-313.

Figure legends

Figure 1. Expression of a functional GFP-tagged ^{WT}FGFR2, ^{SW}FGFR2 and ^{PR}FGFR2.

(A) An immunoblot of the wild type and the Apert mutants (S252W and P253R) from two independently lysed cell extracts of the same clones analyzed with anti-GFP antibody (lanes 1,2 and 3 and lanes 4, 5 and 6 respectively) (upper panel). The immunoblot was stripped and re-probed for Grb2 (a ubiquitous adapter protein in these cells) and shows equivalent levels of Grb2 expression (lower panel). (B) Serum starved cells were incubated with either 3 or 10 ng/ml tunicamycin overnight, cell lysates were prepared and immunoblotted with anti-GFP antibody. (C) Comparative analysis of the level of GFP tagged receptors overexpressed in 293T cells by immunoblotting. 200ng of total cell-lysates from ROS17/2.8 cells with the same amount of lysates serially diluted from ^{WT}FGFR2-GFP expressing cells were loaded in the gel and immunoblotted with anti-FGFR2 antibody (upper panel) and the re-probed with anti-tubulin antibody (lower panel). (D) Quantitative ligand-stimulated tyrosine phosphorylation of the wild type and the Apert mutant receptors indicating the kinase activity of each receptor from three independent experiments. The receptors were immunoprecipitated from 0.5mg of total cell-lysates using 10 µg of anti-GFP antibody and analysed in an immunoblot with the anti-phosphotyrosine antibody. The phosphorylated receptor bands were quantified using densitometry where the unstimulated WT receptor phosphorylation was normalised as 1.0 and the relative increase or decrease in band intensities are shown. Error bar represents standard deviation. (E) Serum starved cells were stimulated with 10 ng/ml FGF9 and cell

lysates were prepared. Total cell-lysates of cells expressing the wild type and the mutants were analysed in an immunoblot with the anti-phosphotyrosine antibody (upper panel), stripped and re-probed with anti-FRS2 antibody (middle panel) and anti-FGFR2 antibody (lower panel). (F) A comparison of the unstimulated and FGF9 stimulated receptor phosphorylation between the wild type FGFR2 (WT) with a C-terminal deletion similar to the K-*sam*-IIC3 (WTΔC) in stably transfected 293T cells. Serum starved cells expressing the wild type FGFR2 and WTΔC were stimulated with 10ng/ml FGF9 for 15min. Cell-lysates were prepared and immunoblotted using anti-phosphotyrosine (upper panel). The band intensity was normalised to the unstimulated WT lane and the relative changes are shown. The immunoblot was re-probed with anti-GFP antibody (middle panel). A longer exposure of the anti-phosphotyrosine blot is shown in the lower panel to demonstrate that the middle receptor band is less phosphorylated.

Figure 2. FGF9 induced co-localization of tyrosine phosphorylated proteins with the wild type and mutants FGFR2.

Stable 293 cells expressing GFP-tagged wild type and mutant FGFR2 were grown on a coverslip, serum starved overnight and stimulated with 10 ng/ml FGF9 for designated time periods. Cells were fixed and counter-stained for tyrosine phosphorylated proteins with pY99-Cy3 antibody. The cellular localization of tyrosine phosphorylated proteins and GFP-tagged receptors are captured using confocal microscope. (A) Localization of the ^{WT}FGFR2, the ^{SW}FGFR2 and the ^{PR}FGFR2 receptors with tyrosine phosphorylated proteins. (B) A control experiment showing the co-localization of the ^{WT}FGFR2 with tyrosine phosphorylated proteins following 15 minutes of 100 nM insulin stimulation.

The confocal image demonstrates that the pY-labelled Cy3 antibody is sufficient to detect tyrosine phosphorylated protein in the cell. Graphs are generated using Leica confocal software is the representation of the fluorescent intensity of each pixel along the drawn line segment.

Figure 3. Time course comparison of ERK activation between ^{WT}FGFR2, ^{SW}FGFR2 and ^{PR}FGFR2 cells.

Serum starved cells expressing ^{WT}FGFR2, ^{SW}FGFR2 and ^{PR}FGFR2 were stimulated with either 10 ng/ml FGF2 or FGF9 for the designated time period. Cells were washed once with PBS and lysed with lysis buffer. (A) Soluble protein (5µg of whole cell lysates) was immunoblotted with an antibody that detects phosphorylated ERK (pERK) (upper panel). The numbers represents the relative band intensity after normalisation to WT 60min (denoted as 1). Blot was stripped and reprobed with anti-ERK (lower panel). (B) Densitometry quantification of the FGF2 stimulated ERK phosphorylation from three independent experiments after normalised to WT 60min as above. (C) Densitometry quantification of the FGF9 stimulated ERK phosphorylation from three independent experiments. Error bars represent standard deviations.

Figure 4. The localization of FRS2 with the wild type and mutant FGFR2 following FGF9 stimulation.

Stable 293T cells expressing GFP-tagged wild type and mutant FGFR2 were transiently transfected with RFP tagged FRS2. Following 24 hours post transfection cells were seeded onto coverslip and allowed to grow a further 48 hours. Cells were serum starved overnight and stimulated with 10 ng/ml FGF9 for designated time, fixed and analysed by

confocal microscopy. (A) Co-localization of the ^{WT}FGFR2-GFP,. ^{SW}FGFR2-GFP and ^{PR}FGFR2-GFP with FRS2-RFP (B) Co-localization of FRS2-RFP with ^{WT}FGFR2 and ^{SW}FGFR2 following 15 minutes insulin stimulation. Showing insulin has no effect on FRS2 localisation thus it is a specific substrate for FGFR2. Furthermore a control experiment showing expression of isolated RFP displaying a distinct pattern of expression compared to when tagged to FRS2.

Figure 5. Co-precipitation of FGFR2 with FRS2.

(A) Serum starved 293T cells expressing ^{WT}FGFR2, ^{SW}FGFR2 and ^{PR}FGFR2 were stimulated with 10 ng/ml FGF9 and whole cell lysates were prepared. FRS2 was precipitated using anti-FRS2 antibody and probed with anti-phosphotyrosine (pY) (upper panel), stripped and re-probed with anti-FRS2 (upper middle panel), anti-FGFR2 (lower middle panel) and IgG level shown in the bottom panel. Minus denotes unstimulated and plus denote 15min FGF9 stimulation. The numbers denote the band intensity normalised to 1.0 using the wild type stimulated lane (B) FRS2 was immunoprecipitated with GST-p13^{suc1} from unstimulated, FGF2 and FGF9 stimulated Ros17/2.8 cells and probed with anti-phosphotyrosine (upper panel). Stripped and re-probed with anti-FGFR2 (upper middle panel), anti-FRS2 (lower middle panel) and anti-GST antibodies (lower panel).

Figure 6. Comparison of direct interaction between FRS2 and the receptors using fluorescence lifetime imaging microscopy.

Stable 293 cells expressing GFP-tagged wild type and mutant FGFR2 were transiently transfected with RFP tagged FRS2. Following 24 hours post transfection cells were seeded onto coverslips and allowed to grow a further 48 hours. Cells were serum starved

overnight and stimulated with 10 ng/ml FGF9 for designated time, fixed and analysed by confocal microscopy. Co-localization of FRS2-RFP with the wild type and the mutants were acquired. The lifetime measurements were made over a 300 second acquisition period as described in the materials and method. The top panel shows the fluorescence intensity image and the middle panel the lifetime data, mapped to an arbitrary colour scale from blue to red. The fluorescence lifetime distribution for all pixels in the field of view is provided on the bottom with the same colour scale. (A) Co-localization and FLIM image of FRS2-RFP with ^{WT}FGFR2-GFP. (B) Co-localization and FLIM image of FRS2-RFP with ^{SW}FGFR2-GFP. (C) Co-localization and FLIM image of FRS2-RFP with ^{PR}FGFR2-GFP. (D) The control lifetime of the GFP and RFP. Graphs represent the average lifetime of entire population of cells seen in the image.

Figure 7. The FGFR2 localize to the lysosome upon FGF9 stimulation.

The wild type FGFR2 stably expressing HEK293T cells grown on a coverslip. Overnight serum starved cells were incubated with LysoTracker Red DND99 dye for 15 minutes and then stimulated with 10ng/ml FGF9 for the designated time period and fixed. The cellular localization of GFP-tagged receptors and lysosome are captured using confocal microscope. The image represents the mid-section of the cells.

Biochemical Journal Immediate Publication. Published on 28 Mar 2008 as manuscript BJ20071594

Ahmed et. al

Figure 1 A

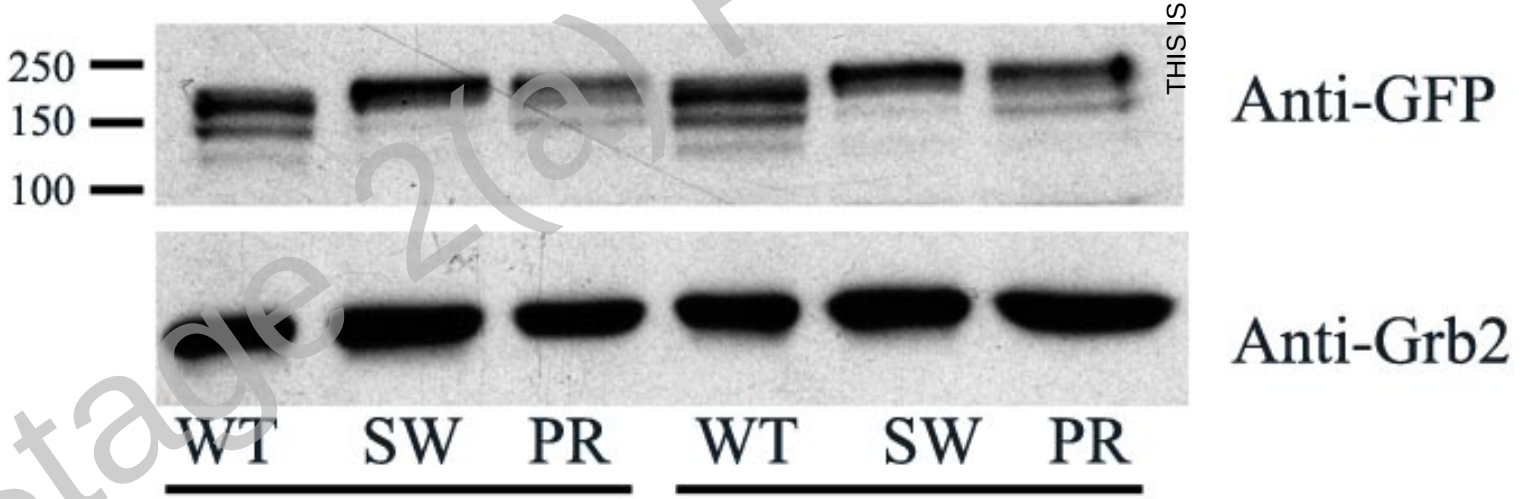

Biochemical Journal Immediate Publication. Published on 28 Mar 2008 as manuscript BJ20071594

Ahmed et. al.

Figure 1 B

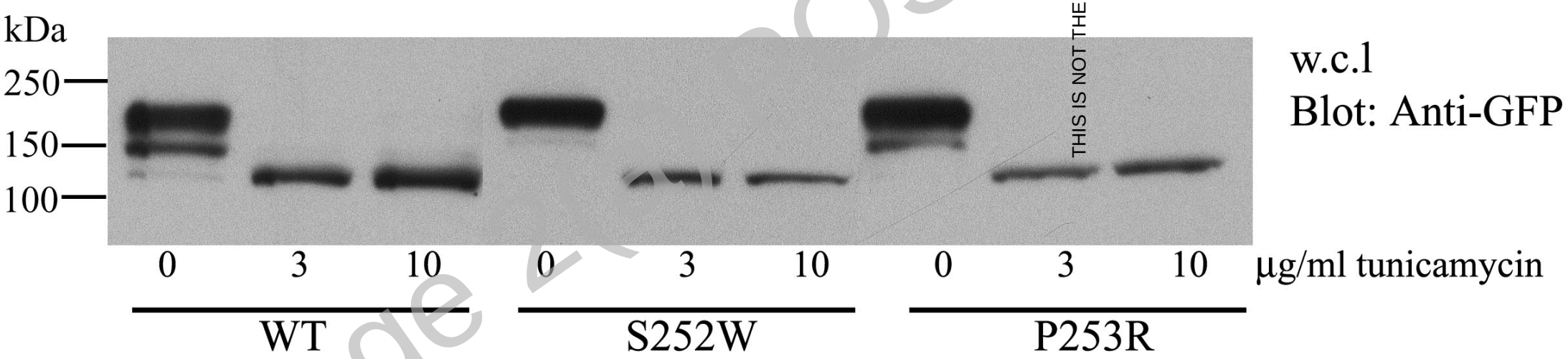

Biochemical Journal Immediate Publication. Published on 28 Mar 2008 as manuscript BJ20071594

Ahmed et. al.

Figure 1C

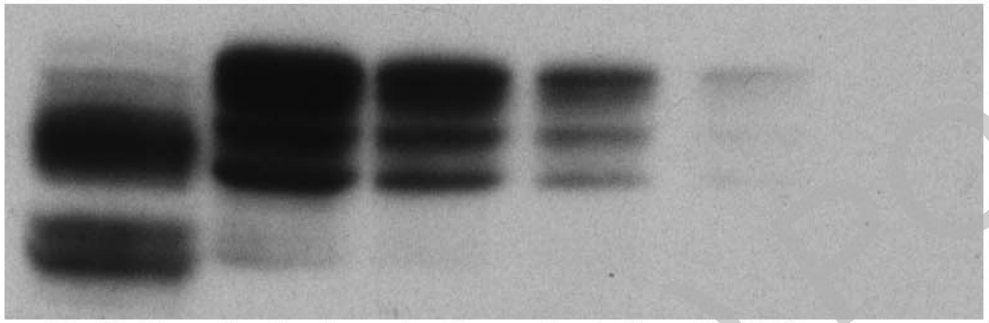

IB: Anti-FGFR2

ROS	1:2.5	1:5	1:10	1:20	Dilution factor
1.0	1.5	0.8	0.4	0.1	Relative band intensity
	3.8	4.0	4.0	2.6	Fould increase in expression

293T-^{WT}FGFR2-GFP

IB: Anti-Tubulin

Biochemical Journal Immediate Publication. Published on 28 Mar 2008 as manuscript BJ20071594

Ahmed et. al.

Figure 1D

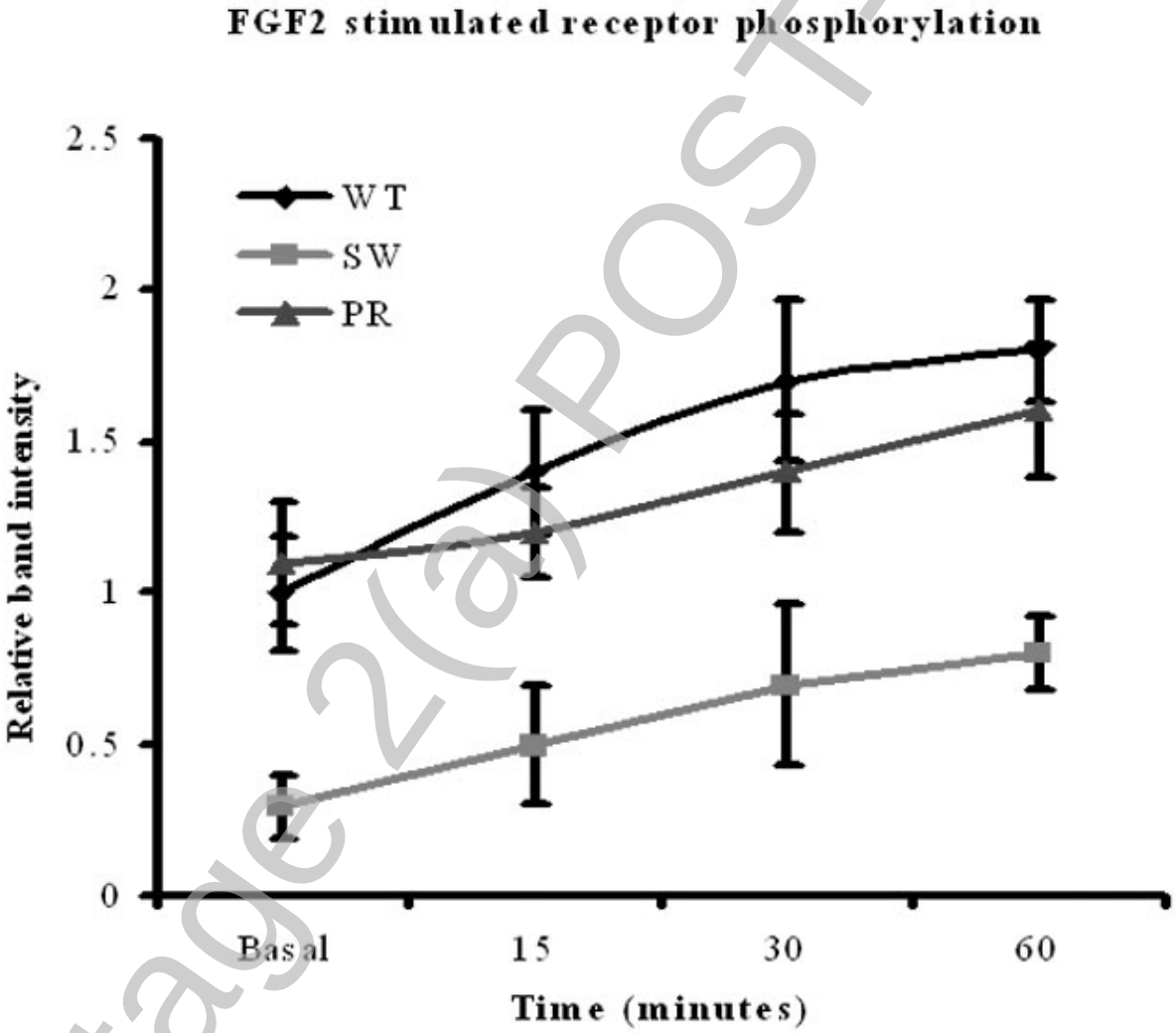

Biochemical Journal Immediate Publication. Published on 28 Mar 2008 as manuscript BJ20071594

Ahmed et. al.

Figure 1E

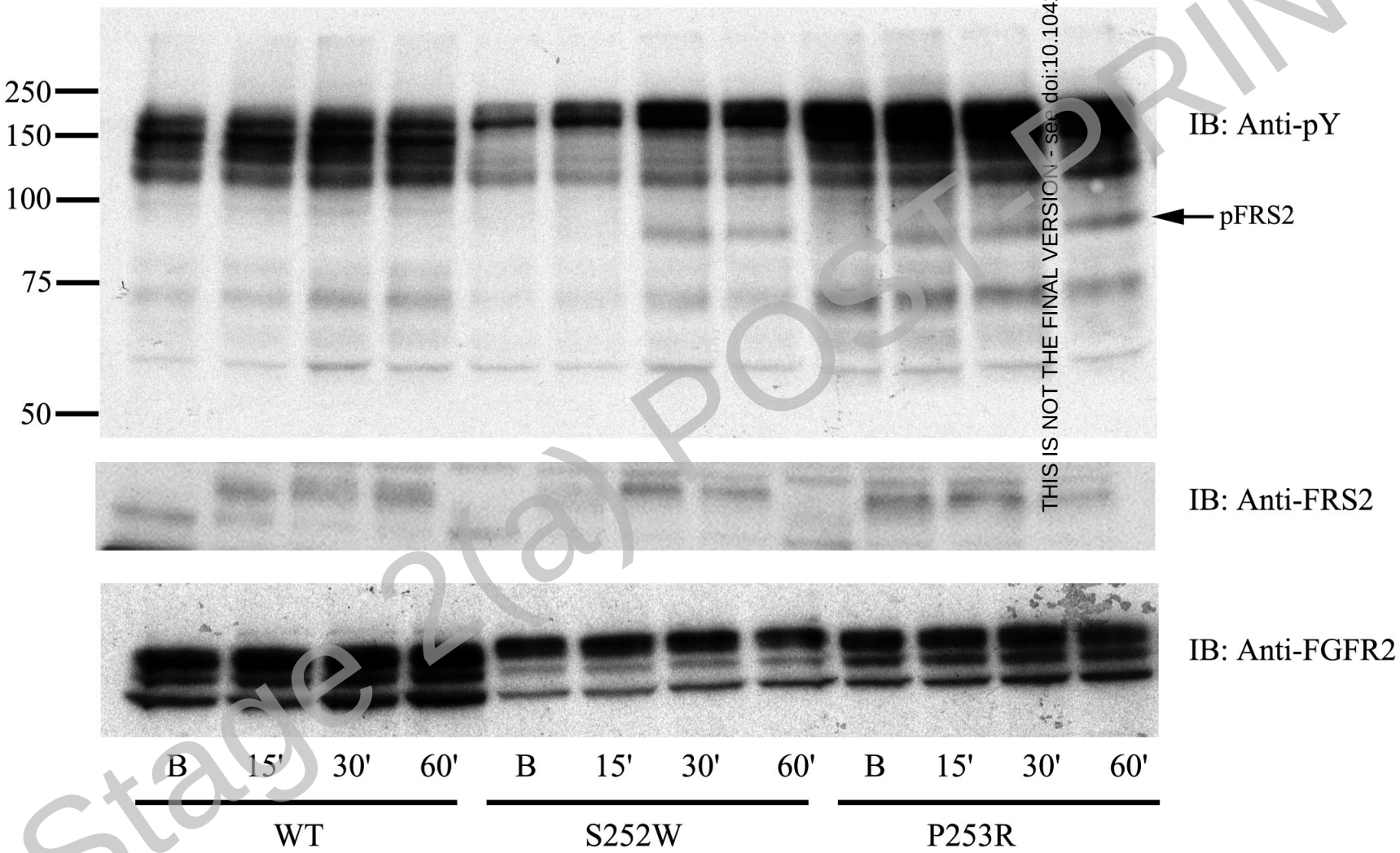

Biochemical Journal Immediate Publication. Published on 28 Mar 2008 as manuscript BJ20071594

Ahmed et. al.

Figure 1F

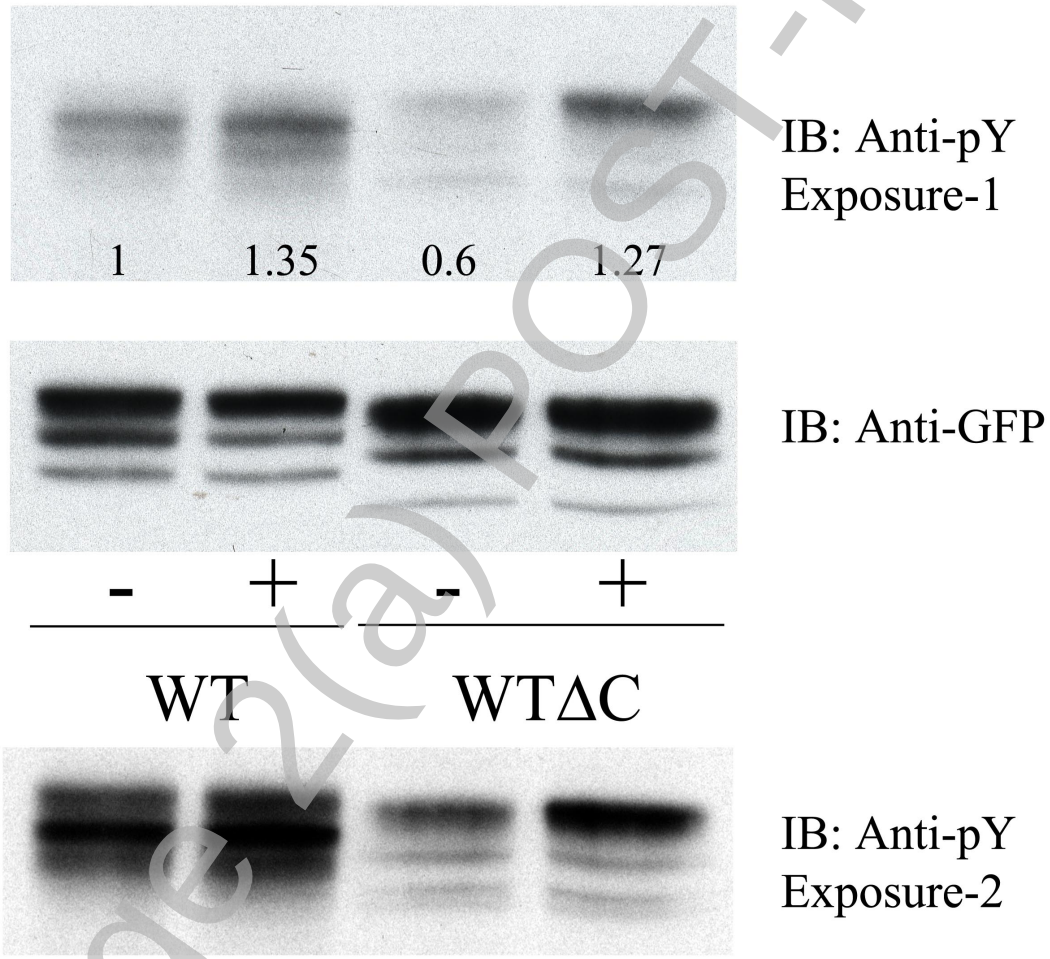

Biochemical Journal Immediate Publication. Published on 28 Mar 2008 as manuscript BJ20071594

Ahmed et. al.

Figure 2 A

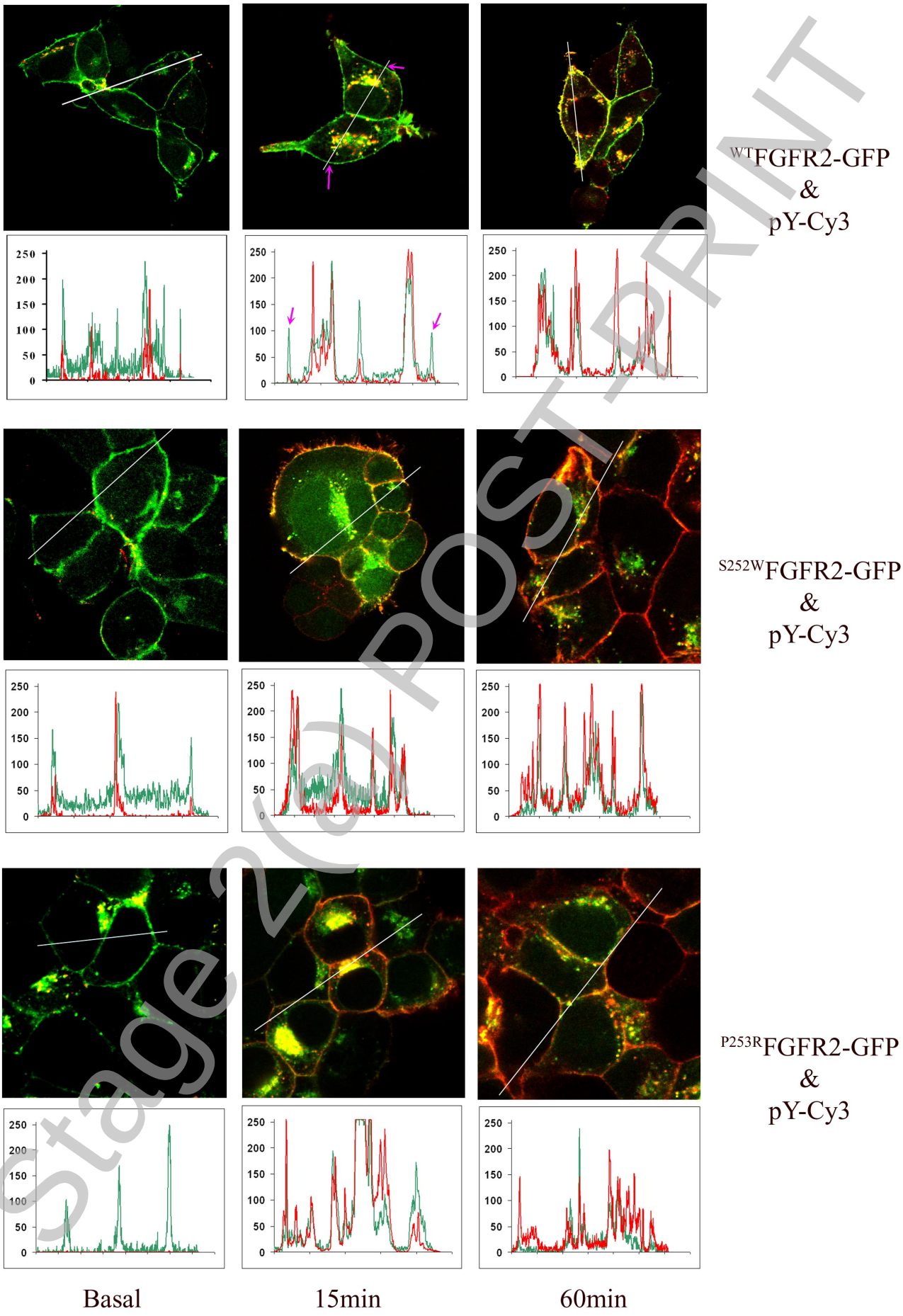

Biochemical Journal Immediate Publication. Published on 28 Mar 2008 as manuscript BJ20071594

Ahmed et. al.

Figure 2 B

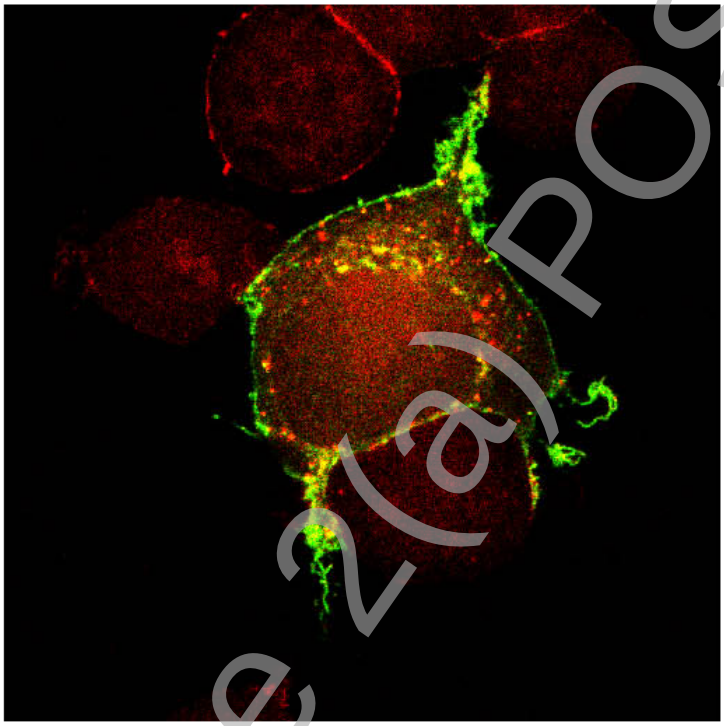

^{WT}FGFR2-GFP

15min Insulin

Figure 3

(A)

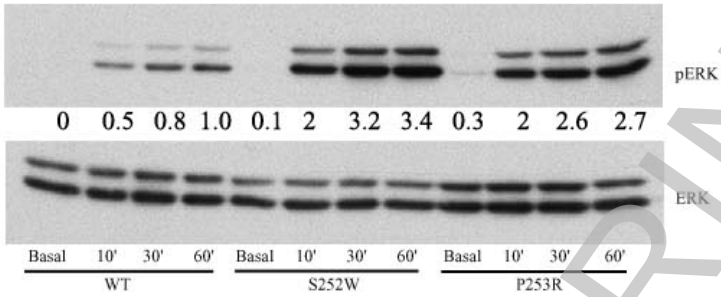

(B)

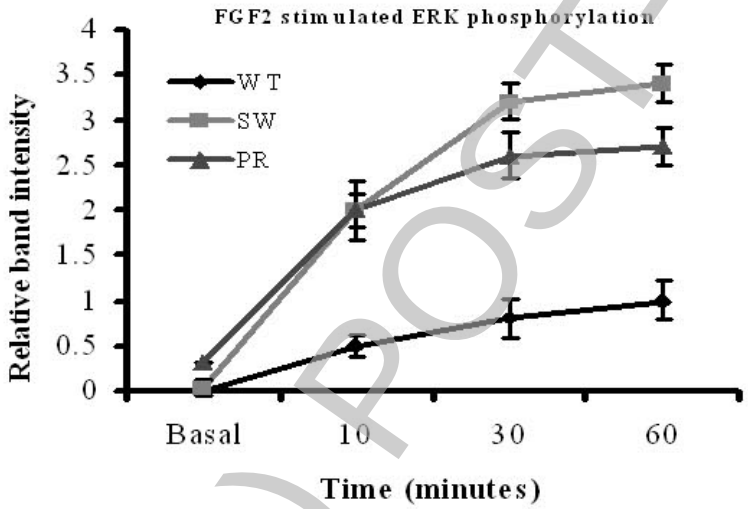

(C)

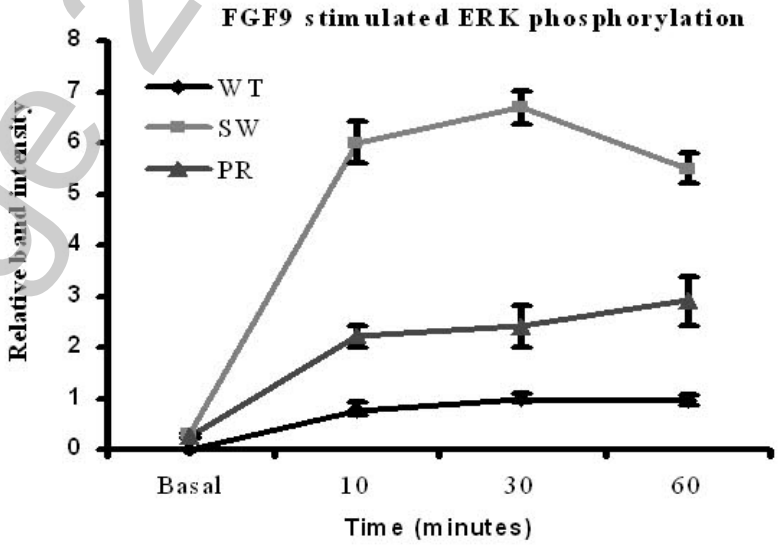

Biochemical Journal Immediate Publication. Published on 28 Mar 2008 as manuscript BJ20071594

Ahmed et. al.

Figure 4 A

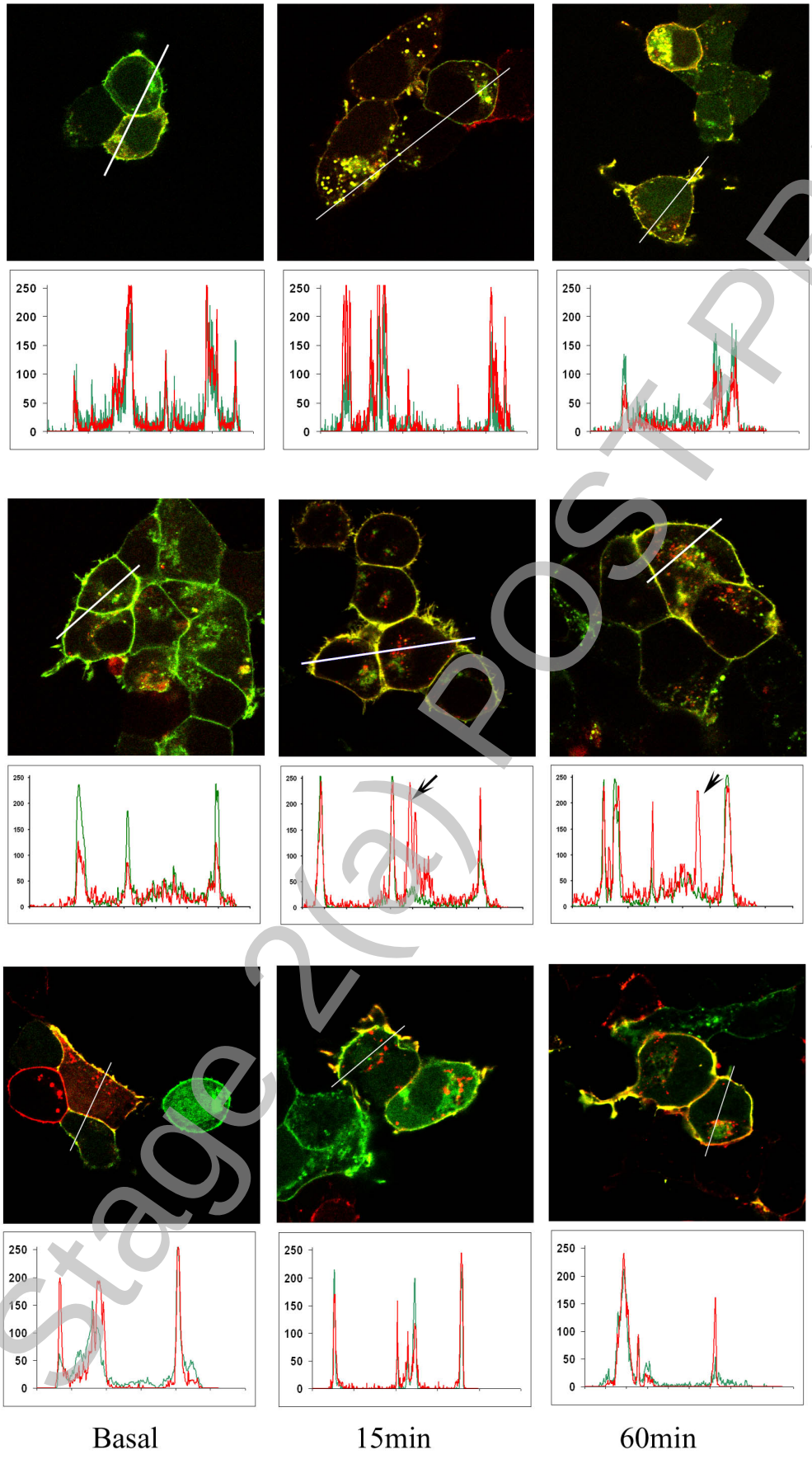

Biochemical Journal Immediate Publication. Published on 28 Mar 2008 as manuscript BJ20071594

Ahmed et. al.

Figure 4 B

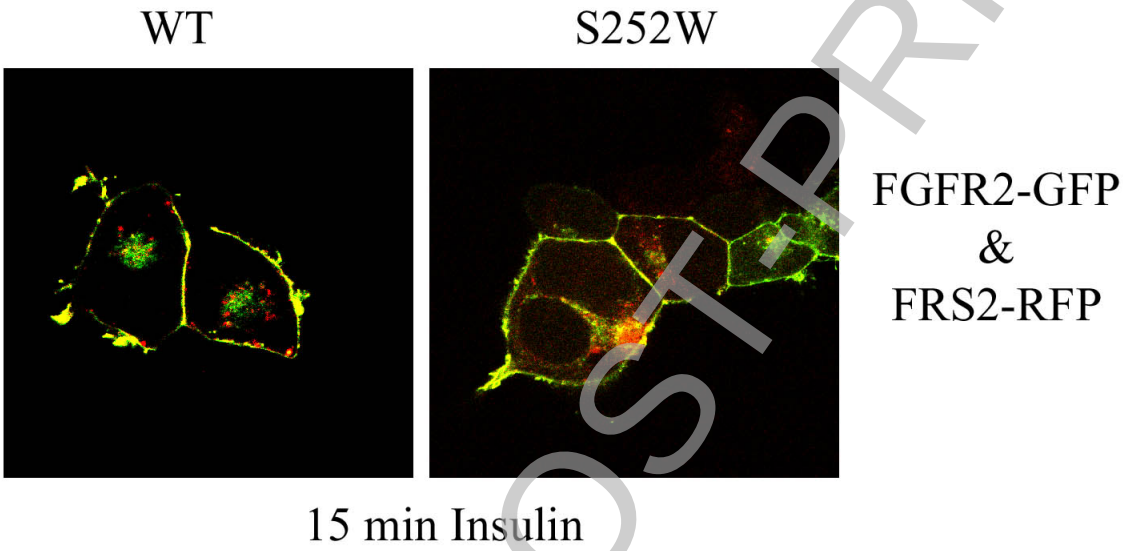

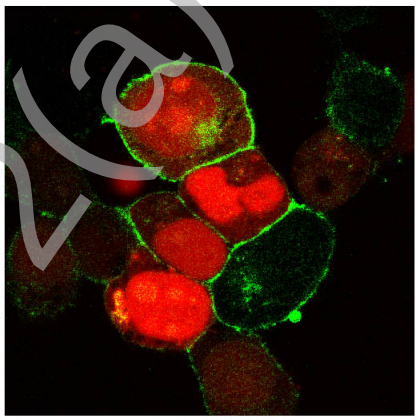

Biochemical Journal Immediate Publication. Published on 28 Mar 2008 as manuscript BJ20071594

Ahmed et. al.

Figure 5A

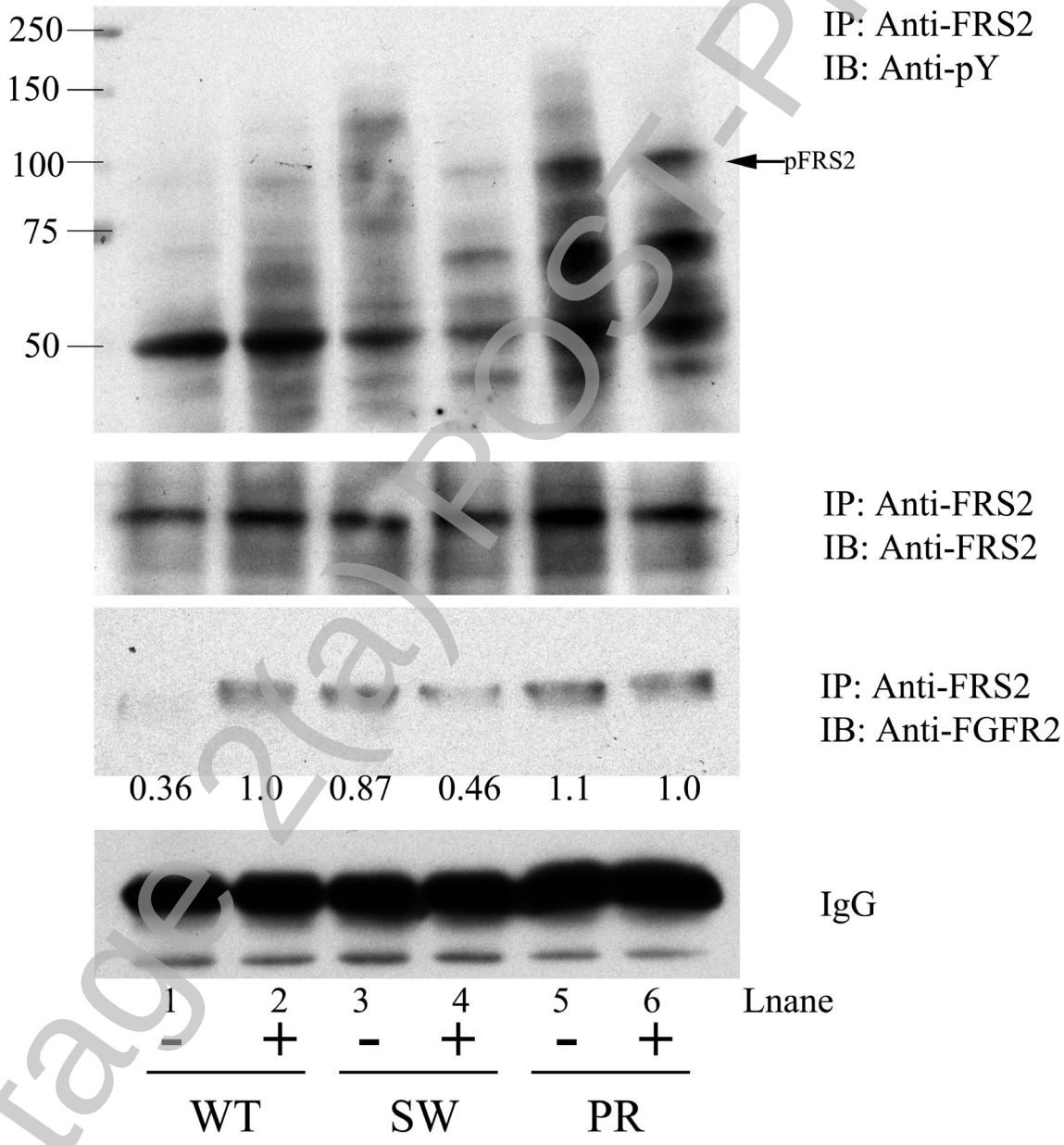

Biochemical Journal Immediate Publication. Published on 28 Mar 2008 as manuscript BJ20071594

Ahmed et. al.
Figure 5B

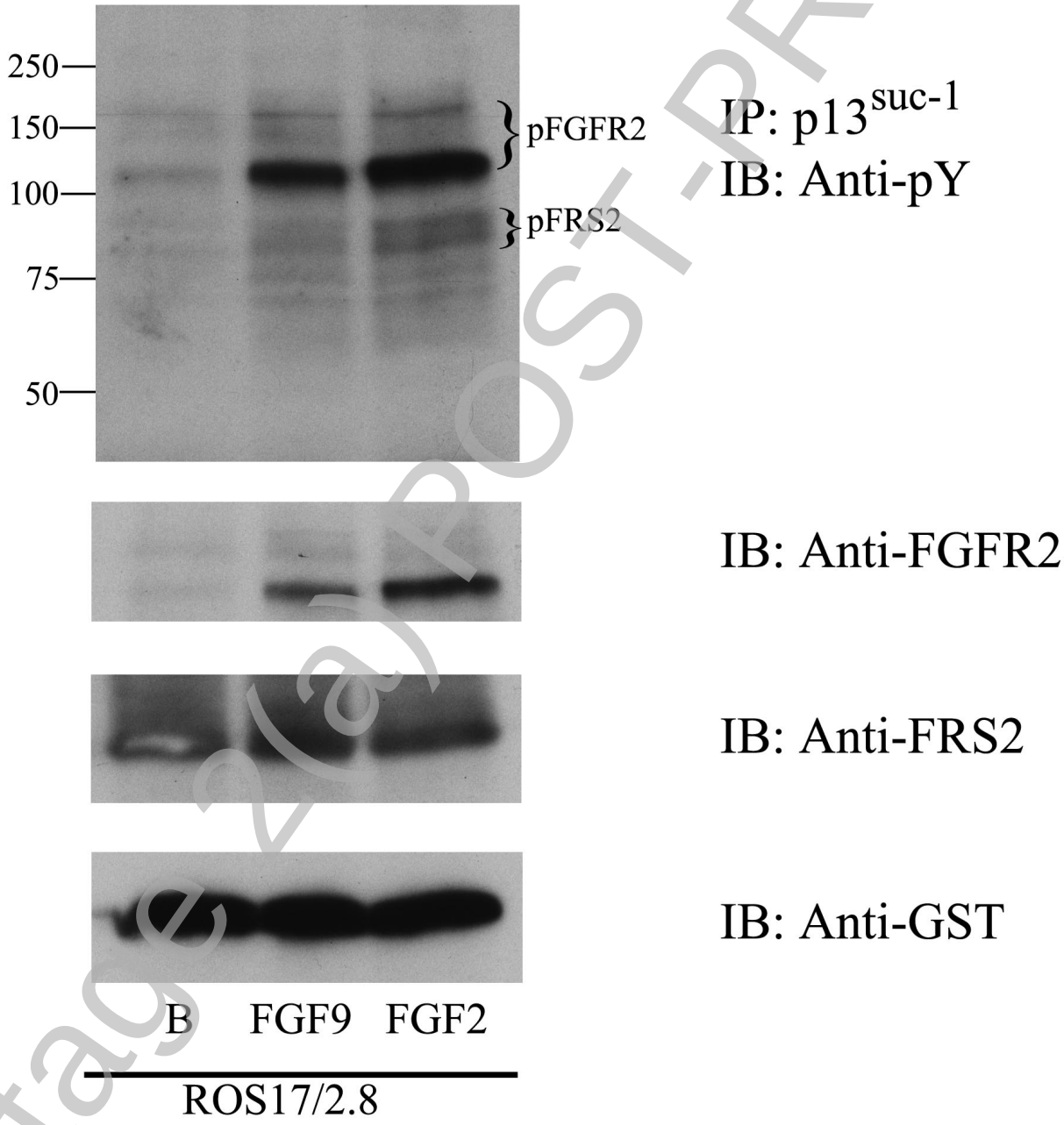

Biochemical Journal Immediate Publication. Published on 28 Mar 2008 as manuscript BJ20071594

Ahmed et. al.

Figure 6 A

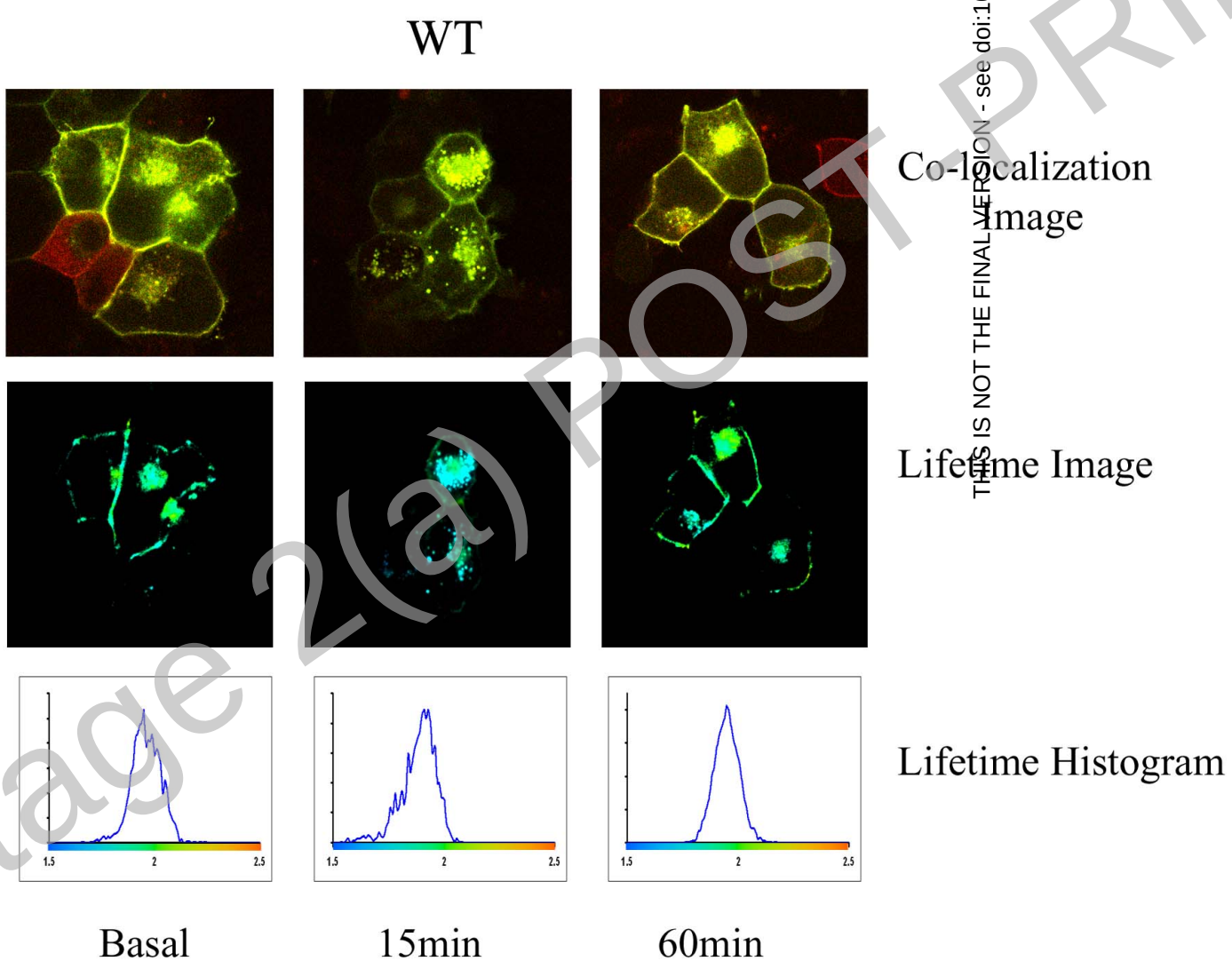

Biochemical Journal Immediate Publication. Published on 28 Mar 2008 as manuscript BJ20071594

Ahmed et. al.

Figure 6 B

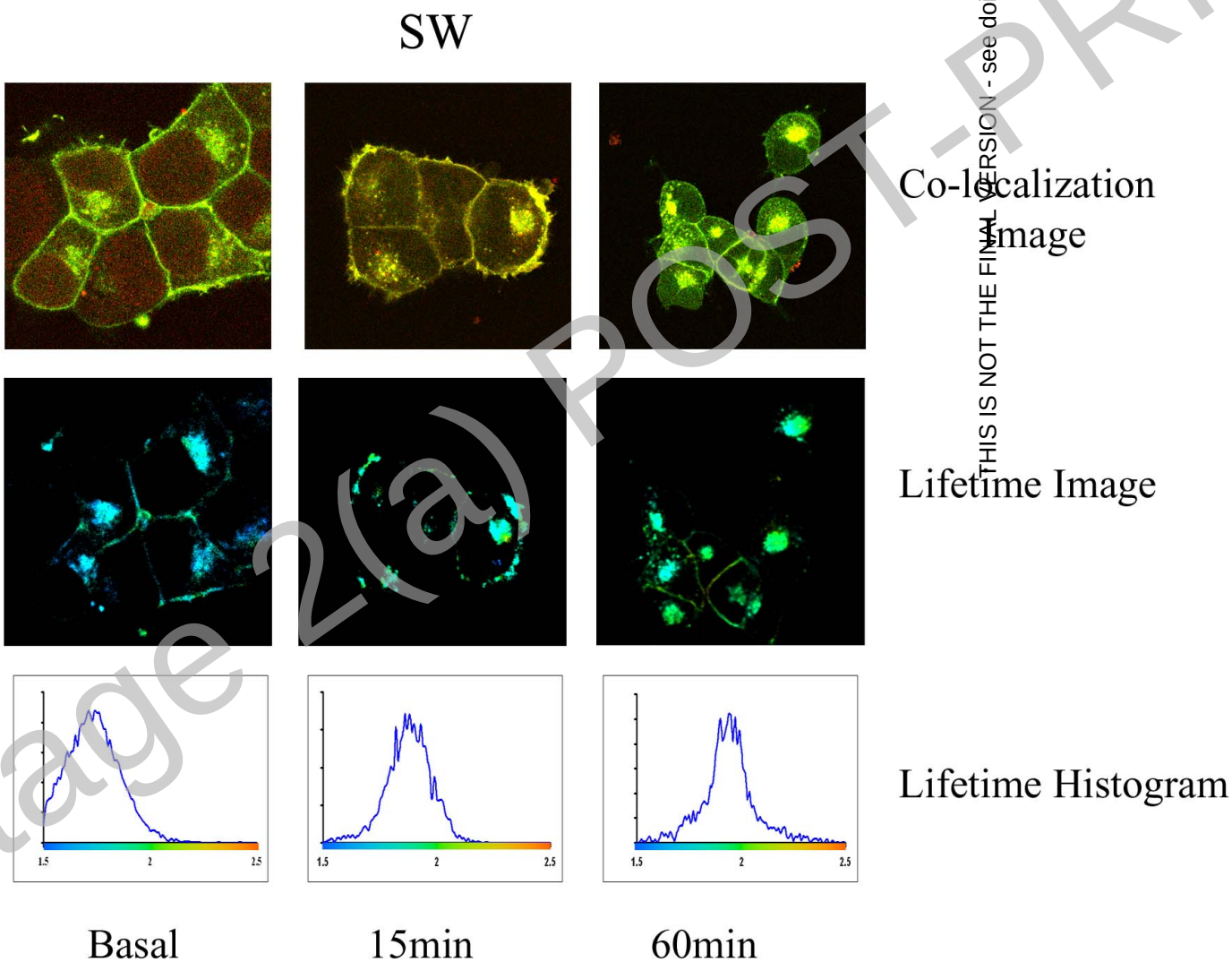

Biochemical Journal Immediate Publication. Published on 28 Mar 2008 as manuscript BJ20071594

Ahmed et. al.

Figure 6 C

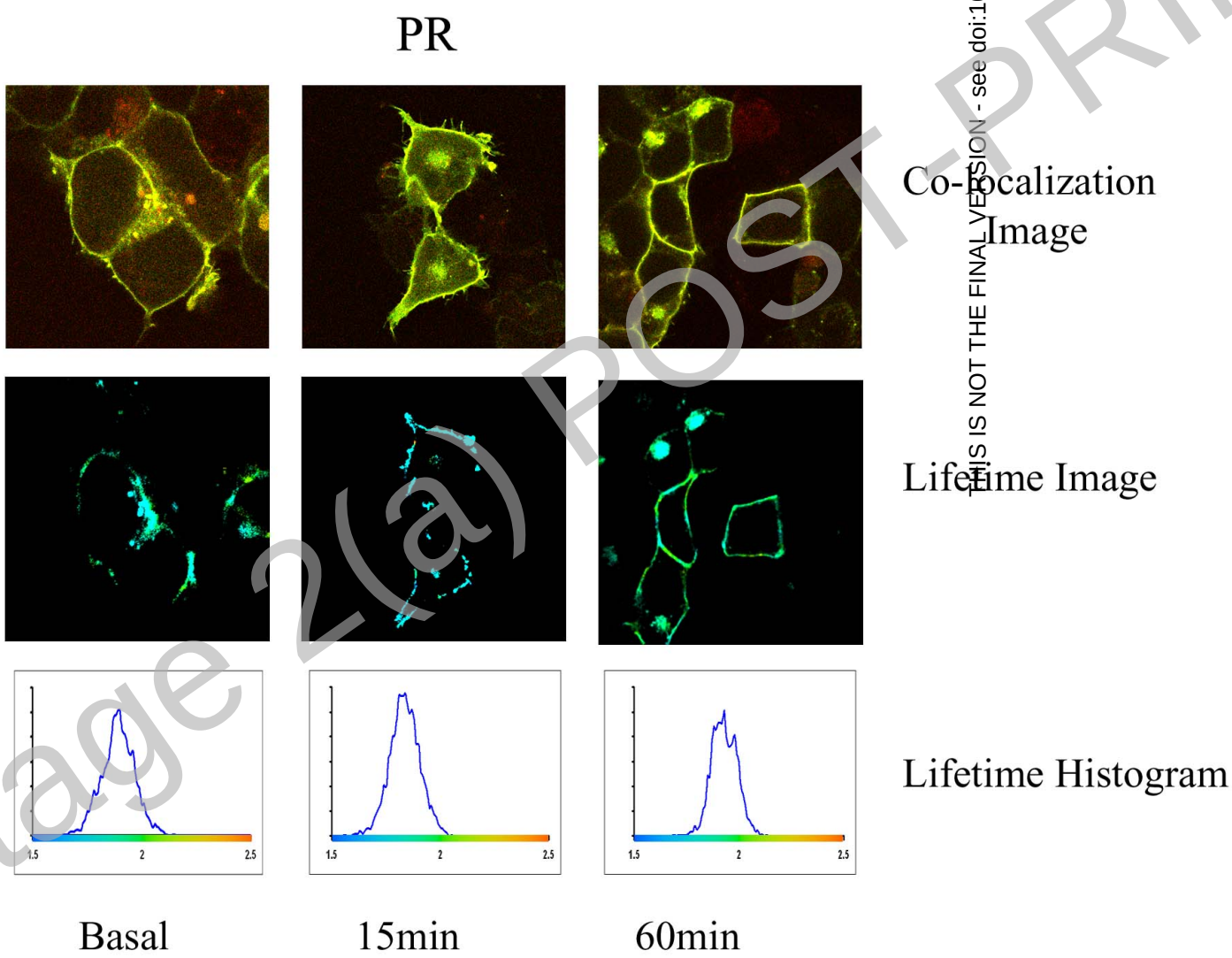

Ahmed et. al.

Figure 6 D

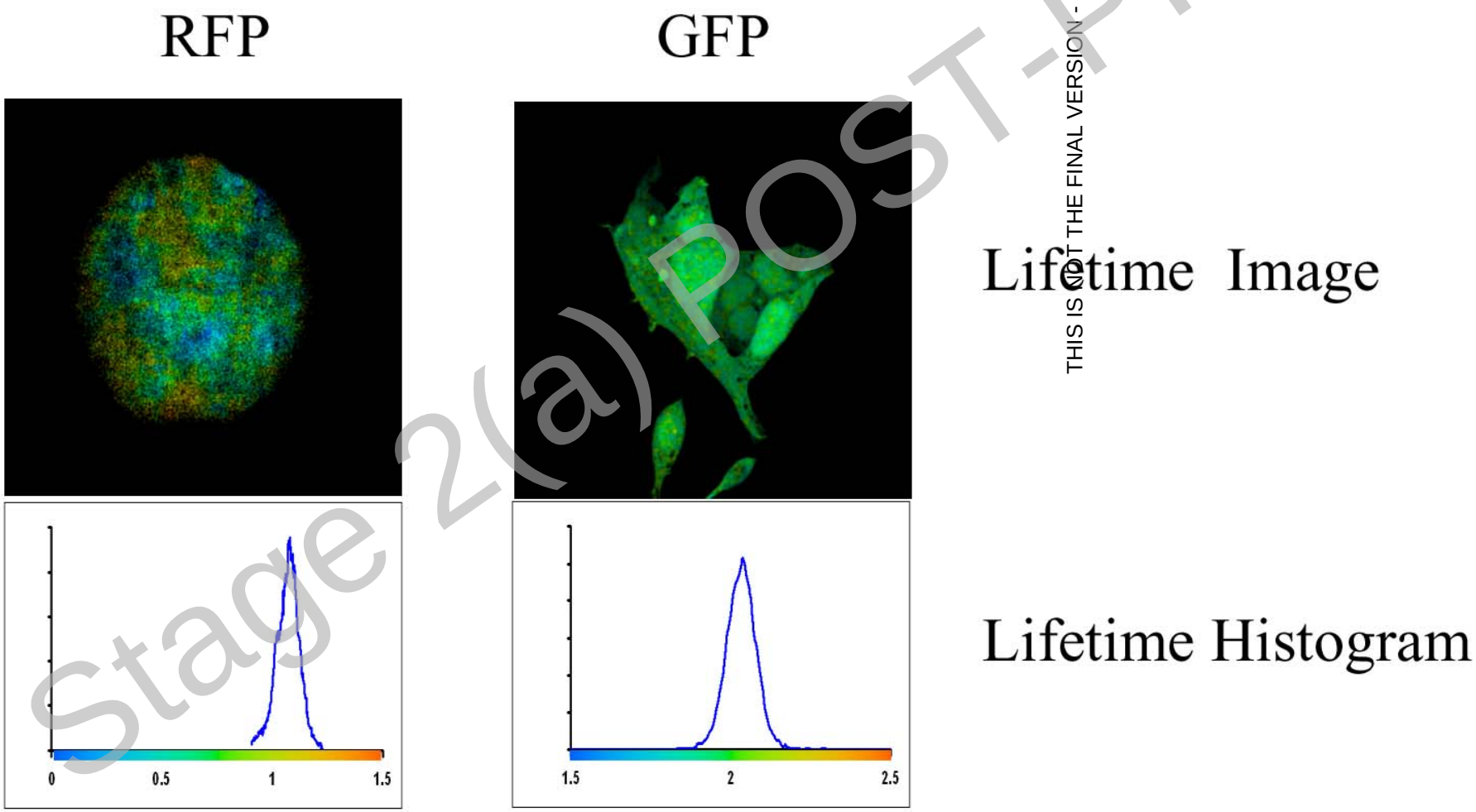

Ahmed et. al.

Figure 7